



PUEY UNGPHAKORN INSTITUTE  
FOR ECONOMIC RESEARCH

# Analysis of Nonlinear Comovement of Benchmark Thai Government Bond Yields

by

Rewat Khanthaporn

July 2022

Discussion Paper

No. 183

The opinions expressed in this discussion paper are those of the author(s) and should not be attributed to the Puey Ungphakorn Institute for Economic Research.

# Analysis of Nonlinear Comovement of Benchmark Thai Government Bond Yields \*

Rewat Khanthaporn †

June 29, 2022

## Abstract

The COVID-19 pandemic is a recent and ongoing extreme event that has impacted all financial markets. Indeed, it impacts the bond or debt market, which is one of the most important financial markets. The main role of the bond market in the economy is to enable the government, firms and institutions to lend and borrow money on acceptable terms and conditions. Since the COVID-19 pandemic began, the bond market has been affected in many different ways including in bond market comovement. For fund firms, emerging market bonds are a vital investment instrument as they tend to offer higher yields than developed market bonds. Hence, this paper analyzes the COVID-19 impact of: 1) nonlinear bivariate comovement between benchmark loan bonds (LBs) in emerging market bonds, in particular the Thai bond market, which is one of the most important Asian bond markets; and 2) nonlinear bivariate comovement between emerging Thai benchmark bonds and developed benchmark bonds in the United States (US), United Kingdom (UK) and Japanese bond markets. An asymmetric generalised autoregressive conditional heteroskedastic (GARCH) model with a mixture of generalised Pareto and Gaussian distributions is applied as a marginal model in step one. Sixteen candidates for a bivariate copula function are fitted and the best fit copula selected in order to obtain numerical nonlinear comovement measures. This is also known as the Inference for the Margins (IFM) method. Empirical results reveal that the COVID-19 pandemic impact in the emerging Thai bond market has characteristics such as in the scale of nonlinear comovement, asymmetric dependence and upper and lower tail dependence. In general, COVID-19 has impacted the comovement between emerging Thai market bonds by increasing the nonlinear comovement, and generating more asymmetric and more extreme upper and lower tail dependence. While emerging Thai market bonds tend to less nonlinear comovement, more symmetric and tail independence are seen with developed market bonds due to the impact of COVID-19.

**Keywords:** Thai Bond Market, COVID-19 pandemic, Copula Dependence Analysis, Asymmetric GARCH, Mixture Distribution, Generalized Pareto Distribution

**JEL Classification:** C22; C63; G12

\*This research was funded by Puey Ungphakron Institute for Economic Research. The author is grateful to acknowledge helpful comments from anonymous reviewers of the Puey Ungphakron Institute for Economic Research. The views in this paper are only the author and do not necessarily represent the views of the funder.

†Email: rewat.khanthaporn@aut.ac.nz. Department of Mathematical Sciences, Auckland University of Technology, Auckland, New Zealand.

## 1 Introduction

The bond market is a financial market where there is a mechanism for the transformation of saving into long term financing for both the government and corporates. In 2019, domestic debt security outstanding value in Thailand's primary market (at par) was 13,304 billion baht with a year-on-year growth rate at 1.70% while debt-to-GDP ratio is about 79%. One of the most essential debt security classes in the Thai bond market, both the primary and secondary markets, is government bonds (LB).

At present, the Thai Government bond yield curve is formulated from survey-based approach by 15 primary bond dealers. Some of them however cannot quote the benchmark bond since changes in compliance policy. In addition, according to the Thai bond market association (ThaiBMA) regulations, if the number of quoted primary dealers is less than threshold, the daily government bond yield curve cannot be generated and the government bond yield curve at time  $t$  will use the previous government bond yield curve at time  $t-1$ . Moreover, at the end of business day, all bond market data will be launched. Given that, the Thai government bond yields will be utilized as a primary input (a risk-free rate) of calculation to the rest and most of the bond market data, for example, mark-to-market (MTM) price, corporate bond yield curve, credit spread curve, state owned enterprise (SOE) spread and so on. This may cause an operational risk in the bond market.

Consequently, ThaiBMA has been initiating an alternative transaction-based approach for the Thai Government bond yield curve in order to prevent operational risk. The transaction-based approach however may face other issues when any benchmark LB has not been traded during the day or it is an illiquid bond, a so-called liquidity risk or an interpolation issue. Hence, understanding illiquid LBs based on available information is required, which may come from traded LBs on that day, so-called bond comovement across tenors or the spillover effect.

Bond common characteristics are spillover and market price volatility effects, the so-called spillover-volatility effect (Christiansen, 2007). One more important bond comovement is the comovement between different bond markets, especially the developed bond market. The Thai bond market is an emerging market and relies significantly on the developed bond markets, for example, the U.S., U.K. and Japanese market. As a result, the investigation of bond market comovement between Thailand and developed countries is essential. Precisely, the study of comovement between Thai Government bonds and others must be explored in order to obtain more market information related to illiquid LB. Furthermore, regarding the current large global economic crisis due to the COVID-19 pandemic (World Bank, 2020), it is worth studying how the COVID-19 crisis affects comovement between the Thai Government bond market and other markets.

Indeed, the study of comovement between LB and the others benefits not only the bond agency but also the market participants, for example, bond dealers, who play a crucial role as a secondary over-the-counter market facilitator and can utilise comovement information for the bid/offer price quotation. Further, from a bond issuer/policy maker/central bank viewpoint, they can use it for their interests, for example, a new bond issue and debt management problem.

In the literature, the copula model has been widely introduced to the study of economic time series comovement, for example, among others, in surveys of [Fan and Patton \(2014\)](#) and [Patton \(2012\)](#). Copula statistics is also in the top two research areas in finance and economics according to [Czado \(2013\)](#). In addition, copula has been broadly extended such as in risk management and portfolio allocation. Section 2 will discuss further details of copula in the literature and, section 3 will discuss further details of the copula model.

Prior to the comovement study, the independence of a time series data analysis is required to extract data residuals. It is clear that the generalised autoregressive conditional heteroscedasticity (GARCH) model has been one of the most important models since Bollerslev introduced it in 1986. Since then, the model has evolved because of its statistical property enrichment. In the literature, an example of a GARCH family is, among others, exponential GARCH (EGARCH), LogGARCH and threshold GARCH (TGARCH) ([Bildirici & Ersin, 2009](#); [Glosten et al., 1993](#); [Hafner & Kyriakopoulou, 2019](#); [Nelson, 1991](#); [Sahamkhadam et al., 2018](#); [Salman Khan et al., 2019](#); [Zakoian, 1994](#)).

The copula model could be fitted to the standardised residuals of the data. In the literature, bivariate elliptical copula and Archimedean copula are well-known and very flexible to the comovement study. It can describe (non-)linear relationships among financial data thanks to Sklar who introduced Sklar's theorem in 1959. For the concepts of copula statistics, see, for example, [Joe \(2015\)](#) and [McNeil et al. \(2015\)](#), pp. 220-274.

Finally, a measure of (non-)linear comovement can be formulated through the Pearson correlation and rank-based method, which is determined by the copula model using Kendall's  $\tau$ , a probability of concordance minus discordance, and Spearman's  $\rho_s$ . However, in the literature, the studies of the copula model in the Thai bond market is still scarce and it indeed requires advanced mathematics.

In conclusion, the study of comovement between the Thai Government bonds across **a**) the tenors and **b**) developed bond markets is required. Besides, it is worth studying the Thai bond market comovement regime-switching due to the impact of the COVID-19 crisis. There are two steps for comovement analysis. Firstly, data residual filtering. Secondly, (non-)linear comovement/dependence measures. The comovement information may more or less support ThaiBMA, the Thai bond agency, for government bond yield curve construction, in particular

for the illiquid government bond yield. Also, it may benefit other bond market participants. For instance, bond dealers can utilise it for bid/offer quotations, bond market monitoring and analysis whereas policy makers or central banks may utilise the information for debt policy implementation. Ultimately, it will promote the money market and economy of Thailand.

## 2 Literature review

Sklar proposed Sklar's theorem in 1959 for the application of copula. Sklar's theorem states that every multivariate cumulative distribution function (cdf) of a random vector can be expressed in terms of its marginals and a copula function. Many scholars propose the analysis of a dependence structure model in various applications such as civil engineering, medicine, hydrology research, geodesy, climate, weather research and finance, and especially in financial risk management. Copula becomes popular among quantitative scholars and practitioners because of its time-varying dependence-structure characteristic fulfilment between two time series.

The bivariate parametric copula model becomes a crucial and well-known model to describe the dependency among financial data characteristics because it successfully describes (non-)linear relationships between assets, (see, among others, [Chang et al. \(2018\)](#)'s survey). There are two main bivariate parametric copulas in the literature as follows:

- ♠ The elliptical parametric copula family
- ♠ The Archimedean parametric copula family including one-parameter and two-parameters

The elliptical copula family consists of the Gaussian and the Student's t copula. There are four most important one-parameter Archimedean copulas; the Clayton, the Gumbel, the Frank and the Joe copulas, whilst more the complicated two-parameters Archimedean copula consists of, for example, the BB1, BB6, BB7 and BB8 copulas.

Among others, elliptical and one-parameter Archimedean copulas were studied by [Brymann et al. \(2003\)](#) in a study of bivariate deseasonalised dependence structures in currency markets. [Berger \(2013\)](#) studied elliptical copulas, dynamic-conditional-correlation and extreme value theory model in 2013. Later, [Kakouris and Rustem \(2014\)](#) applied both elliptical and one-parameter Archimedean copula to the robust portfolio risk optimisation problem and [So and Yeung \(2014\)](#) studied elliptical copula to the solution of necessary conditions via time-varying without the limitation of the linear correlation method and applied it to multivariate cases. Moreover, [De Lira Salvatierra and Patton \(2015\)](#) applied elliptical and one-parameter Archimedean copula to generalised autoregressive score with the realised measures model (GRAS) and ARMA-GJR-GARCH model with a skewed-t innovation. [Babaei et al. \(2015\)](#) also applied elliptical and one-parameter Archimedean copulas to the dynamic stochastic model up to 200 stocks on the S&P500 index. [Creal and Tsay \(2015\)](#) adapted only elliptical copulas

to study a class of comovement time-varying in high dimensional models in equity and credit default swaps (CDS) of the S&P500 index.

In 2016, among others, Oh and Patton explored bivariate copula together with GARCH-dynamic-conditional-correlation (GARCH-DCC), stochastic volatility and heterogeneous autoregressive (HAR) for high-dimensional copula-based distributions with mixed frequency data on the S&P500 market. Fengler and Okhrin proposed a realised copula family among three competing models including GJR-GARCH-DCC, Dynamic copula and GAS/GRAS in their study of portfolio risk management on the NASDAQ and NYSE stock exchange. [Al Janabi et al. \(2017\)](#) applied the GARCH family and copula as well plus both constant conditional correlation (CCC) and DCC to cope with the problem of investment portfolio allocation and multiple constraints.

Research in copula risk management still continually interests scholars. In [2018](#), Segnon and Trede proposed a new model of t-copula-Markov switching multifractal approach to the NASDAQ and the S&P500 for market risk portfolio evaluation. Vine copula with mixture of bivariate one-parameter Archimedean copula together with ARMA-GJR-GARCH model were studied again in a portfolio risk optimisation problem in the study of [Goel et al. \(2019\)](#). [Sahamkhadam et al. \(2018\)](#) studies both elliptical and one-parameter Archimedean copulas plus the asymmetric-GARCH-Extreme-Value-Theorem (EVT) to portfolio risk forecasting. Furthermore, [Li and Kang \(2018\)](#) presented all three main bivariate copulas including elliptical, one-parameter and two-parameters Archimedean copulas incorporated into the GARCH and ACDP (Autoregressive Conditional Double Poisson) model so as to better tail distribution forecasting performance based on five stocks on the NASDAQ stock exchange. [Karmakar and Paul \(2018\)](#) approached all the three main copula families to model ARMA, CGARCH (component generalised autoregressive conditional heteroscedasticity) and EVT to solve Value-at-Risk (VaR) and Expected shortfall (ES) in a high-frequency portfolio risk strategy.

The estimation method is another vital key in order to obtain a robust and superior result of comovement study. To my best knowledge, the maximum likelihood approach (MLE) is a popular approach in the literature. An essential part of the MLE mechanism is the joint density function, called the likelihood function. In the past decade of research, MLE approaches have been used to estimate model parameters, for example, among others, [Berger \(2013\)](#), [Weiß and Supper \(2013\)](#), [Babaei et al. \(2015\)](#), [Fengler and Okhrin \(2016\)](#), [Sahamkhadam et al. \(2018\)](#), [Bernardi and Catania \(2018\)](#) and [Goel et al. \(2019\)](#). It is worth mentioning that bivariate copulas and MLE algorithms do not perform well, in terms of robustness and accuracy, in case of high-dimension time series. A pair-copula construction (or vine copula) and other alternative estimation algorithms, which are Bayesian approaches, might be required for a high-dimension

dependence model. However, it requires far more advances in mathematics and calculation.

In this proposed study, we will focus on the bivariate copula both elliptical and Archimedean copula model and the asymmetric-GARCH model as they commonly appear an approach in the literature. We will also extend these models in order to explore better model fitting for government bond market data. Further, we will determine the other innovations (any other mixtures, especially, in EVT distribution) and Archimedean copula (any other classes of Archimedean copula) that could improve model performance for the Thai bond market comovement analysis of Thailand.

### 3 Methodology

#### 3.1 Finite mixture distribution

This subsection explains statistical properties of finite and countable mixture distribution as an innovation of our proposed conditional volatility model. In statistics, mixture distribution can be represented by either a finite set of cdf  $P_i(z_t)$  or density function (pdf)  $p_i(z_t)$ . Hence, mixture distribution and density function are as a sum, respectively, such that

$$F_i(z_t) = \sum_{i=1}^n w_i P_i(z_t), \quad (1)$$

$$f_i(z_t) = \sum_{i=1}^n w_i p_i(z_t). \quad (2)$$

where weight  $w_i > 0$ ,  $\sum w_i = 1$  and  $i = 1, \dots, n$ . In financial time series, mixtures are applied and are very popular because they can capture the asymmetrical-fat-tail behaviour of financial data also known as EVT and the method is known as peak over threshold (POT). The POT method can simply be integrated with the GARCH family including, for example, the EGARCH, LogGARCH and GJR-GARCH process. This study proposes a mixture of the density based on two (or more) density functions such that the Gaussian distribution for middle part and the generalised Pareto (GPD) distribution, which is one of the main distributional models in POT in EVT, for the lower and upper tail or two-sided. Hence, the proposed mixture distribution is

$$p_i(z_t) = \begin{cases} \frac{1}{\beta^L} \left(1 + \xi^L \frac{(z_t - \mu^L)}{\beta^L}\right)^{-\frac{1}{\xi^L} - 1}, & z_t \leq \Phi^{-1}(a) \\ \phi(z_t), & \Phi^{-1}(a) < z_t < \Phi^{-1}(b) \\ \frac{1}{\beta^U} \left(1 + \xi^U \frac{(z_t - \mu^U)}{\beta^U}\right)^{-\frac{1}{\xi^U} - 1}, & z_t \geq \Phi^{-1}(b) \end{cases} \quad (3)$$

where  $a$  and  $b$  are a probability or quantile.  $-\infty < \mu < \infty$  is a location parameter,  $0 < \beta < \infty$  is a scale parameter,  $-\infty < \xi < \infty$  is a shape parameter. The support of  $z_t$  of GPD is  $z_t \geq 0$  when  $\xi \geq 0$  and  $\mu \leq z_t \leq \mu - \beta$  when  $\xi < 0$ ,.  $0 \leq \xi < 0.5$  represents a fat tail.  $z_t$  exists at least up to the second moment. The GPD consists of, in the sense of generalisation, an ordinary Pareto distribution when  $\xi > 0$ , an exponential distribution when  $\xi = 0$  and a short-tailed, Pareto type II distribution when  $\xi < 0$ . Denote that  $X \sim GPD(\mu, \beta, \xi)$ , therefore,  $E(X) = \mu + \frac{\beta}{1-\xi}$ ,  $\xi < 1$  and  $var(X) = \frac{\beta^2}{(1-\xi)^2(1-2\xi)}$  when  $\xi < 0.5$ . While  $\phi(\cdot)$  and  $\Phi^{-1}(\cdot)$  are the pdf and inverse cdf of the Gaussian function, respectively. Note that **mixture** in equation 3 will be applied to our proposed conditional volatility model in the next subsection 3.2.

### 3.2 Conditional volatility model: GARCH family

Two step approaches are implemented in this study. This is referred to as the Inference for the Margins method (IFM) (Al Janabi et al., 2017, for example). **Firstly**, univariate (asymmetric-)GARCH models with mixture innovation will be formulated to search for the best model fitting of government bond datasets in order to obtain the standardised residuals. Note that this GARCH family also fulfils volatility clustering, non-normality and fat-tails properties, which are crucial characteristics of financial time series. See Engle (2004) for a survey. Example of research papers, among others, are Cai (1994), Hamilton and Susmel (1994), Gray (1996), Bauwens et al. (2010), Francq et al. (2013), So and Yeung (2014), Neumeyer et al. (2019), Billio et al. (2016), Ardia et al. (2018), Francq et al. (2018) and Hafner and Kyriakopoulou (2019). **Secondly**, a comovement measure between the Thai Government bond yields across tenors and comovement measure between Thai government bond and developed bond markets such those the U.S., U.K., and Japanese bond market will be calculated. There are three GARCH-type processes in this study including the classical GARCH process and other two asymmetric-GARCH processes, which are Exponential-GARCH (EGARCH) process and LogGARCH process.

#### 3.2.1 GARCH process

A crucial model in financial time series analysis is the conditional volatility model. Clearly that generalised autoregressive conditional heteroscedasticity model, the GARCH family, is one of the most crucial in conditional volatility models since Bollerslev (1986) evolved the GARCH model. Let a financial yield series denoted by  $\{y_t\}$ ,  $y_t = \varepsilon_t = \sqrt{h_t}z_t$ ,  $t \in \mathbb{Z}$ . GARCH(p,q) process is

$$h_t = \omega + \sum_{i=1}^p \alpha_i \varepsilon_{t-i}^2 + \sum_{j=1}^q \nu_j h_{t-j} \quad (4)$$



where  $\{z_t\}$  is a vector of independent, identically distributed (iid) random variables with zero mean and unit variance,  $h_t$  is conditional volatility and  $F_{t-1}$  – *measurable*, where  $F_{t-1}$  is the  $\sigma$  – *algebra* generated by the past information up to time  $t-1$ , and the innovation term  $\varepsilon_t$  is a zero mean and conditional volatility  $h_t$ .  $p \geq 0, q > 0, \omega > 0, \alpha_i \geq 0, \nu_j \geq 0, 0 \leq \alpha_i + \nu_j \leq 1, 1 \leq i \leq p, 1 \leq j \leq q$  and  $p, q \in \mathbb{Z}$  to ensure that the conditional volatility  $h_t$  is almost surely strictly positive or a strictly stationary process; for details, see, among others, [Oh and Patton \(2016\)](#). Given the parameter space  $\Theta$ , the estimated parameter of the GARCH(p,q) is  $\hat{\Theta} := \{\hat{\omega}, \hat{\alpha}_i, \hat{\nu}_j, 1 \leq i \leq p, 1 \leq j \leq q\}$ . For simplicity, we study the GARCH family's lags including the innovation term and the volatility term when  $p = 1$  and  $q = 1$  since more lags of them is much less popular in the literature.

### 3.2.2 Exponential-GARCH process

Popularity of the asymmetric-GARCH family in the research area of the volatility model reflects how importance of the GARCH family because it responds to the crucial financial return characteristic such as volatility clustering and non-normality. The exponential-type GARCH models are one of the leading extensions of the asymmetric GARCH family. The well-known exponential-type GARCH process is the exponential-GARCH(p,q,r) or EGARCH(p,q,r) of [Nelson \(1991\)](#) given by

$$\log h_t = \omega + \sum_{i=1}^p \gamma_i z_{t-i} + \sum_{j=1}^q \delta_j |z|_{t-j} + \sum_{k=1}^r \nu_k \log h_{t-k} \quad (5)$$

where the conditional volatility is log volatility rather than volatility. Given the parameter space  $\Theta$ , the estimated parameter of the EGARCH(p,q,r) is  $\hat{\Theta} := \{-\infty \leq \hat{\omega}, \hat{\gamma}_i, \hat{\delta}_j \leq \infty, |\hat{\nu}_k| < 1, 1 \leq i \leq p, 1 \leq j \leq q, 1 \leq k \leq r\}$ . The "news impact" function  $g(z_{t-1})$  of the EGARCH model is  $\omega + \sum_{i=1}^p \gamma_i z_{t-i} + \sum_{j=1}^q \delta_j |z|_{t-j}$  term while  $\nu_k$  is the volatility persistence parameter.  $\gamma$  and  $\delta$  are implied the shock asymmetry and the size effect, respectively. If  $\gamma > 0$ , positive shocks increase volatility more than negative shocks of the same size and vice versa.

### 3.2.3 LogGARCH process

Another popular exponential-type GARCH process is LogGARCH(p,q) (For model details, see, for example, in [Francq et al. in 2019](#)) given by

$$\log h_t = \omega + \sum_{i=1}^p (\alpha_i^+ I_{\{\varepsilon_{t-i} > 0\}} + \alpha_i^- I_{\{\varepsilon_{t-i} < 0\}}) \log \varepsilon_{t-i}^2 + \sum_{j=1}^q \nu_j \log h_{t-j}, \quad t \in \mathbb{Z} \quad (6)$$

where  $I$  is an indicator function,  $\alpha^+ + \alpha^- + \nu < 1$  and  $\nu + \frac{1}{2}[|\alpha^+| + |\alpha^-|] < 1$ . Given the parameter space  $\Theta$ , the estimated parameter of the LogGARCH (p,q) is  $\hat{\Theta} := \{\omega, \alpha_i^+, \alpha_i^-, \nu_j, 1 \leq i \leq p, 1 \leq j \leq q\}$ . The "news impact" function of the LogGARCH is the term of  $\omega + \sum_{i=1}^p (\alpha_i^+ I_{\{\varepsilon_{t-i} > 0\}} + \alpha_i^- I_{\{\varepsilon_{t-i} < 0\}}) \log \varepsilon_{t-i}^2$ . When  $\alpha_i^- = \alpha_i^+$  represents symmetric Log-GARCH process. The LogGARCH has a well-known problem which is if the  $\varepsilon_{t-i}$  term equal to zero. It therefore will mean that the conditional volatility cannot be generated.

For a discussion of the LogGARCH process, see, among others, in [Weiß and Supper \(2013\)](#), [Salman Khan et al. \(2019\)](#), and [Sucarrat et al. \(2016\)](#). For the reviews of the exponential-type GARCH, please see, among others, [Joe \(2015\)](#), [Hentschel \(1995\)](#) and [Jose Rodriguez and Ruiz \(2012\)](#) and a recent study of the exponential-type GARCH process, see, among others, in [Weiß and Supper \(2013\)](#), [Chang et al. \(2018\)](#), [Li and Kang \(2018\)](#) and [Bildirici and Ersin \(2009\)](#).

### 3.3 Nonlinear comovement measure: Bivariate copula model

This section presents as follows: list of sixteen bivariate parametric copula function including Elliptical copula family, Archimedean copula family, BB copula family and nonlinear copula-based dependence measures including Kendall's  $\tau$  and Spearman's  $\rho_s$ .

#### 3.3.1 Elliptical copula model

The elliptical copulas are the Gaussian copula and the Student's t copula. In general case, the multivariate distribution copulas of the Gaussian and the Student's t, respectively, are

$$\begin{aligned} C_{\Sigma}^{Ga}(u) &= \Phi_{\Sigma}(\Phi^{-1}(u_1), \dots, \Phi^{-1}(u_d)) \\ C_{v, \Sigma}^t(u) &= t_{v, \Sigma}(t_v^{-1}(u_1), \dots, t_v^{-1}(u_d)) \end{aligned} \quad (7)$$

where  $\Phi^{-1}$  is an inverse cumulative Gaussian distribution or inverse cdf.  $\Sigma$  is a  $d \times d$  correlation matrix and  $\Sigma$  is equal to  $\rho$  when it is bivariate elliptical copula,  $d = 2$ .  $u_i \sim Unif(0, 1)$  is a continuous standard uniform random variable for all  $i = 1, \dots, d$ .  $t^{-1}$  is an inverse cumulative student's t distribution or inverse cdf.  $t_{v, \Sigma}$  is the cdf of multivariate  $t_{v, \Sigma}$  distribution where  $v > 2$  degree of freedom.

#### 3.3.2 One and two-parameter Archimedean copula models

All one-parameter and two-parameter copula families for our study are as follows. One-parameter Archimedean copulas are Clayton, Frank, Gumbel, Galambos and Joe/B5 whereas two-parameter Archimedean copulas are BB1, BB3, BB4, BB5, BB6, BB7, BB8, BB9 and BB10 which come from the relevant copula in the literature. For all cdf copulas and their properties, see [Joe \(2015\)](#), Chapter 4 and the Archimedean cdf copula shows in Table 1. Note

Table 1: Archimedean parametric copula family

Name of Copula	Bivariate Copula $C(u, v), 0 \leq u, v \leq 1$	Parameter $\theta, \delta$
<b>One-parameter</b>		
Gumbel	$\exp[-((-\log(u))^\theta + (-\log(v))^\theta)^{1/\theta}]$	$\theta \geq 1$
Clayton	$[max(u^{-\theta} + v^{-\theta} - 1, 0)]^{-1/\theta}$	$\theta \geq -1, \theta \neq 0$
Frank	$-\frac{1}{\theta} \ln \left( 1 + \frac{(e^{-\theta u} - 1)(e^{-\theta v} - 1)}{e^{-\theta} - 1} \right)$	$-\infty < \theta < \infty, \theta \neq 0$
Joe/B5	$1 - [(1-u)^\theta + (1-v)^\theta - (1-u)^\theta(1-v)^\theta]^{1/\theta}$	$\theta \geq 1$
Galambos	$uv \exp\{[(-\log u)^{-\theta} + (-\log v)^{-\theta}]^{-1/\theta}\}$	$0 \leq \theta < \infty$
<b>Two-parameters</b>		
BB1	$(1 + [(u^{-\theta} - 1)^\delta + (v^{-\theta} - 1)^\delta]^{1/\delta})^{-1/\theta}$	$\theta > 0, \delta \geq 1$
BB3	$\exp\{-[\delta^{-1} \log(e^{\delta \tilde{u}^\theta} + e^{\delta \tilde{v}^\theta} - 1)]^{1/\theta}\}, \tilde{u} = -\log(u), \tilde{v} = -\log(v)$	$\theta \geq 1, \delta > 0$
BB4	$(u^{-\theta} + v^{-\theta} - 1 - [(u^{-\theta} - 1)^{-\delta} + (v^{-\theta} - 1)^{-\delta}]^{-1/\delta})^{-1/\theta}$	$\theta \geq 0, \delta > 0$
BB5	$\exp\{-[x^\theta + y^\theta - (x^{-\theta\delta} + y^{-\theta\delta})^{-1/\delta}]^{1/\theta}\}, x = -\log(u), y = -\log(v)$	$\theta \geq 1, \delta > 0$
BB6	$1 - (1 - \exp\{-[(-\log(1 - \tilde{u}^\theta))^\delta + (-\log(1 - \tilde{v}^\theta))^\delta]^{1/\delta}\})^{1/\theta}, \tilde{u} = 1 - u, \tilde{v} = 1 - v$	$\theta \geq 1, \delta \geq 1$
BB7	$1 - (1 - [(1 - \tilde{u}^\theta)^{-\delta} + (1 - \tilde{v}^\theta)^{-\delta} - 1]^{-1/\delta})^{1/\theta}, \tilde{u} = 1 - u, \tilde{v} = 1 - v$	$\theta \geq 1, \delta > 0$
BB8	$\delta^{-1}(1 - \{1 - \eta^{-1}[1 - (1 - \delta u)^\theta][1 - (1 - \delta v)^\theta]\})^{1/\theta}, \eta = 1 - (1 - \delta)^\theta$	$\theta \geq 1, 0 < \delta \leq 1$
BB9	$\exp\{-[(\delta^{-1} - \log(u))^\theta + (\delta^{-1} - \log(v))^\theta - \delta^{-\theta}]^{1/\theta} + \delta^{-1}\}$	$\theta \geq 1, \delta > 0$
BB10	$uv[1 - \delta(1 - u^\theta)(1 - v^\theta)]^{-1/\theta}$	$\theta > 0, 0 \leq \delta \leq 1$

that the Archimedean cdf copula is  $C(u, v) = \varphi(\varphi^{-1}(u) + \varphi^{-1}(v))$ . It is worth mentioning that  $C(u, v; \theta, \delta) = G(x, y; \theta, \delta)$  where  $G(x, y; \theta, \delta)$  is a bivariate survival function and  $x, y$  are monotone decreasing transforms. Therefore, the conditional cdf and copula pdf are:

$$C_{2|1}(v|u; \theta, \delta) = \frac{\partial G}{\partial x} \cdot \frac{\partial x}{\partial u} \quad (8)$$

$$c(u, v; \theta, \delta) = \frac{\partial^2 G}{\partial x \partial y} \cdot \frac{\partial x}{\partial u} \cdot \frac{\partial y}{\partial v}$$

### 3.3.3 Copula-based dependence measure

This section shows a rank-based measurement of dependence from which we will formulate Kendall's  $\tau$  and Spearman's  $\rho_s$ . Table 2 shows the closed form of dependence measure of the copula family for this study. In case the closed form solution of dependence measure of the copula family does not exist, we can estimate them using numerical approximation via a Monte-Carlo simulation through two-variable integrals as in equation 9 for Kendall's  $\tau$  and equation 10 for Spearman's  $\rho_s$ , respectively. Note that an example of Gaussian dependence measure is demonstrated in Figure 1.

$$\hat{\tau}(C) = 1 - 4 \int_0^1 \int_0^1 C_{1|2}(u|v)C_{2|1}(v|u)dudv \quad (9)$$

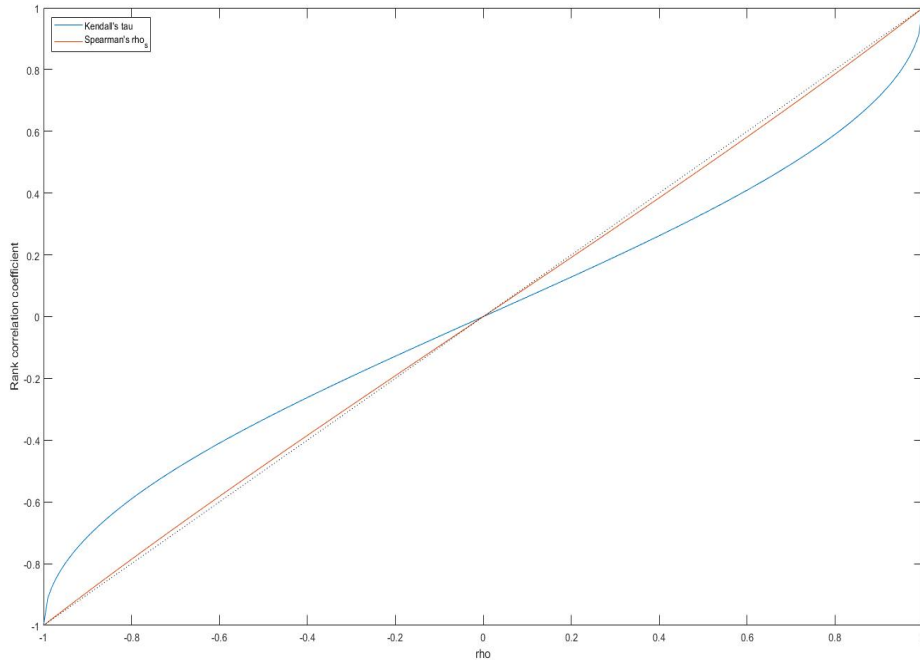
$$\hat{\rho}_s(C) = 3 - 12 \int_0^1 \int_0^1 uC_{2|1}(v|u)dudv \quad (10)$$

Table 2: Closed form solution of Kendall's  $\tau$  and Spearman's  $\rho_s$  against linear correlation coefficient  $\rho$  of copula family

Name of Copula	Kendall's $\tau$	Spearman's $\rho_s$
Gaussian	$2\pi^{-1} \arcsin(\rho)$	$6\pi^{-1} \arcsin(\rho/2)$
t	$2\pi^{-1} \arcsin(\rho)$	$6\pi^{-1} \arcsin(\hat{\rho}/2), \hat{\rho} = 2B((\rho+1)/2, a(\nu), a(\nu)) - 1$
Gumbel	$(\theta-1)/\theta$	Matlab function or Equation 10
Clayton	$\theta/(\theta+2)$	Matlab function or Equation 10
Frank	$1 + 4\theta^{-1}[D_1(\theta) - 1]$	$1 + 12\theta^{-1}[D_2(\theta) - D_1(\theta)], D_k(x) = kx^{-k} \int_0^x t^k (e^t - 1)^{-1} dt$
Joe/B5	$1 - 2(2-\theta)^{-1}[\psi(2) - \psi(2/\theta+1)]$	Equation 10
BB1	$1 + 2/(\delta(\theta+2))$	Equation 10

Note.  $B$  is incomplete beta function and  $a(\nu)$  is Spearman's  $\rho_s$  approximation for a t copula with  $\nu$  degrees of freedom.  $\psi$  is digamma function.

Figure 1: Kendall's  $\tau$  and Spearman's  $\rho_s$  against linear correlation coefficient  $\rho$  of bivariate Gaussian copula



### 3.4 QMLE estimation method

The estimation method is crucial in order to obtain a robust parameter estimator. In this study we consider the quasi-maximum likelihood method (QMLE) which is well-known and commonly appears in the literature, see, among others, [Hafner and Kyriakopoulou \(2019\)](#), [Sahamkhadam et al. \(2018\)](#) and [Francq et al. \(2013\)](#).

#### 3.4.1 Likelihood function

In statistics, the likelihood function measures the goodness of fit of a mathematical model among data observations for the set of unknown parameter(s),  $\Theta$ . It is a joint probability. Thus, likelihood function is

$$L(\Theta) = \prod_{t=1}^T f(y_t|\Theta). \quad (11)$$

In practice, we take the log of the likelihood function as it is computationally simpler and easier to optimise. It is worth mentioning that to maximise the log likelihood function we use the *fmincon* function in the optimisation toolbox of MATLAB<sup>®</sup>. The log likelihood function  $\Lambda(\Theta)$  is

$$\Lambda(\Theta) = \sum_{t=1}^T \log(f(y_t|\Theta)). \quad (12)$$

Following our proposed GARCH processes, let  $z_t = y_t/\sqrt{h_t}$ . To standardise the mixture innovation in equation 3, we set  $\beta = (1 - \xi) / (1 - 2\xi)^{1/2}$ . Therefore, the log likelihood function of this GARCH family with the mixture is

$$\begin{aligned} \Lambda(\Theta) &= \sum_{t=1}^T \log[ap_L^{GPD}(z_t) + (1 - 2a)p^G(z_t) + ap_U^{GPD}(z_t)] \\ p_L^{GPD}(z_t) &= \frac{1}{\sqrt{h_t}(1 - \xi^L)(1 - 2\xi^L)^{1/2}} \left( 1 + \frac{\xi^L y_t}{\sqrt{h_t}(1 - \xi^L)(1 - 2\xi^L)^{1/2}} \right)^{-\frac{1}{\xi^L} - 1}, \\ p^G(z_t) &= \frac{1}{(2\pi h_t)^{1/2}} \exp\left[\frac{-y_t^2}{2h_t}\right], \\ p_U^{GPD}(z_t) &= \frac{1}{\sqrt{h_t}(1 - \xi^U)(1 - 2\xi^U)^{1/2}} \left( 1 + \frac{\xi^U y_t}{\sqrt{h_t}(1 - \xi^U)(1 - 2\xi^U)^{1/2}} \right)^{-\frac{1}{\xi^U} - 1} \end{aligned} \quad (13)$$

where weight  $a$  is a proportion of pdf or quantile,  $h_t$  is conditional volatility.  $h_t$  can be our three proposed GARCH processes with mixture innovation. Hence, parameter estimators of, for example, GARCH(1,1)-mixture are  $\hat{\Theta} = \{\hat{\omega}, \hat{\alpha}, \hat{\nu}, \hat{\xi}^L, \hat{\xi}^U\}$ . Note that the quantile  $a$  can be defined as the left and right boundary of distribution or a pre-specified quantile where we set  $a$  equal to 0.10. Again, it is worth mentioning that our proposed models can fulfill two important financial data stylised facts: volatility clustering and non-normal distribution (fat-tails and asymmetric distribution).

#### 3.4.2 Our estimation step

There are two steps of method in order to obtain Kendall's  $\tau$  and Spearman's  $\rho_s$  dependence values. The steps and their explanation using QMLE estimation method are

**Step 1** We estimate the model parameters for univariate (asymmetric-)GARCH-mixture models in equation 4, equation 5 and equation 6 with the mixture innovation, equation 13. Then, we choose the best fitting model. The example of model parameter  $\hat{\Theta}$  of EGARCH(1,1,1)-mixture model is  $\hat{\Theta} = \{\hat{\omega}, \hat{\gamma}, \hat{\delta}, \hat{\nu}, \hat{\xi}^L, \hat{\xi}^U\}$ . Note that blocking of estimation may be required if a convergence issue occurs. After that, we perform data standardisation.

**Step 2** Given standardised data  $z_t$ , we estimate the copula parameter in Table 1 and also select the best fitting copula model. Finally, we calculate the copula-based dependence measure given by the best fitting copula model.

All proposed models in **Step 1** will be developed in MATLAB<sup>®</sup> while, for **Step 2** models, we will use the MATLAB<sup>®</sup> function for the Gaussian, Student's t, Clayton, Gumbel and Frank copula and copula-based dependence measures, Kendall's  $\tau$  and Spearman's  $\rho_s$ . Otherwise, the BB1, BB2, BB3, BB4, BB5, BB6, BB7, BB8, BB9 and BB10, we will develop in MATLAB<sup>®</sup>.

#### 4 Model comparison

To compare across models, we calculate the mean absolute deviation (MAD), root mean squared error (RMSE), mean absolute percentage error (MAPE), Akaike information criterion (AIC) and Bayesian information criterion (BIC) to assess the model performance and a two-sample Kolmogorov-Smirnov (KS) test for the out-of-sample forecasts (Bildirici & Ersin, 2009; So & Yeung, 2014). Note that the KS test is used to assess whether the forecast distribution is close to the empirical one. The higher the p-value, the closer the forecast distribution is. The model performance is calculated as follows:

Mean Absolute Deviation (MAD):

$$MAD = \frac{1}{T} \sum_{t=1}^T |\hat{y}_t - y_t|$$

Root Mean Square Error (RMSE):

$$RMSE = \sqrt{\frac{1}{T} \sum_{t=1}^T (\hat{y}_t - y_t)^2}$$

Mean Absolute Percentage Error (MAPE):

$$MAPE = \frac{1}{T} \sum_{t=1}^T \left| \frac{y_t - \hat{y}_t}{y_t} \right|$$

Akaike information criterion (AIC) and Bayesian information criterion (BIC), respectively:

$$AIC = -2\loglik(\hat{\theta}_{obs}) + 2(n)$$

$$BIC = -2\loglik(\hat{\theta}_{obs}) + n\log(n)$$

where  $\loglik$  is log likelihood function given by estimated parameters and  $n$  is number of parameters. The smaller AIC or BIC values are considered as the better model. Two-sample Kolmogorov-Smirnov (KS) test is a nonparametric hypothesis test that evaluates the difference between the two sample data, the test statistic is

$$D^* = \sup_t (|\hat{F}(t) - F(t)|)$$

where  $\hat{y}_t$  is a forecast data.  $y_t$  is actual data.  $F_i(t)$  is a cdf function. For more details, see [Massey \(1951\)](#).

## 5 Data collection and preliminary data analysis

We illustrate our proposed models along with the benchmark Thai Government bond yields (Thai LB yields) and developed bond markets including the US, UK and Japanese bond market including the 1 month (1M), 3 months (3M), 6 months (6M), 1 year (1Y), 5 years (5Y), 10 years (10Y), 20 years (20Y) and 30 years (30Y). The full daily dataset period is between January 2010 and April 2021 and the dataset are retrieved from the Thai Bond Market Association (ThaiBMA) and Investing website. For the COVID-19 impact bond market comovement analysis purpose, we split the data into pre-COVID-19 pandemic period and during-COVID-19 pandemic period such that

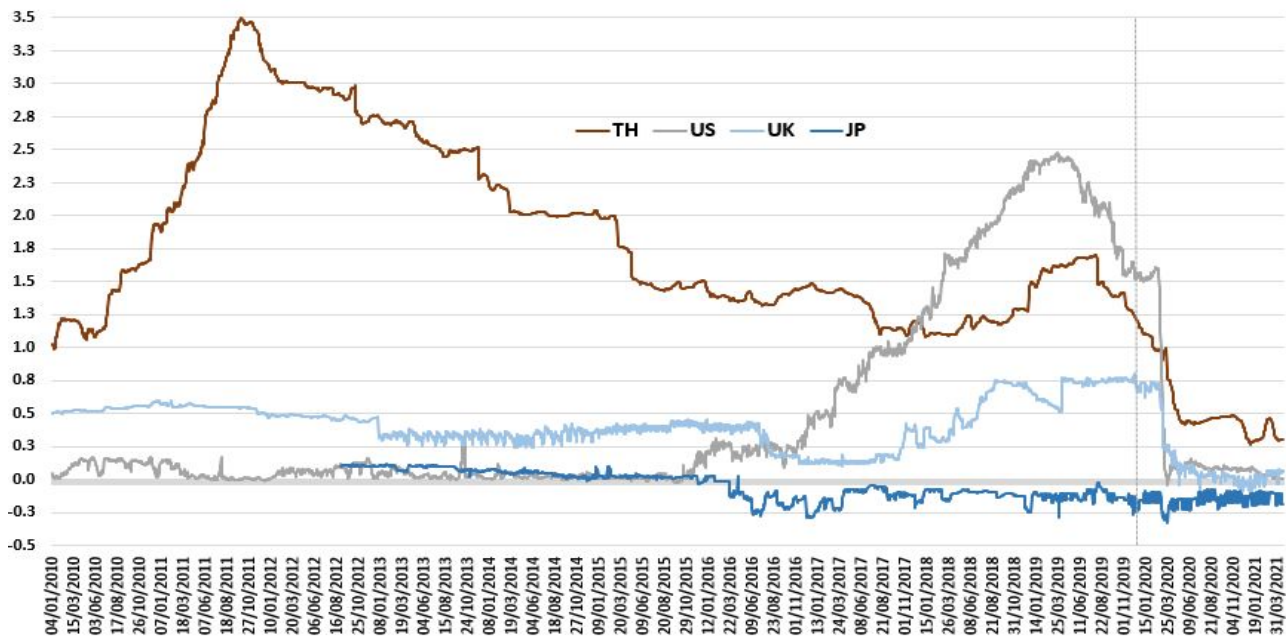
1. **Pre-COVID-19 pandemic period** is from January 2010, to avoid the effect of the 2008 financial crisis, to 17 November 2019. Yet, the data between 2 July 2010 and 26 October 2010 of 30-year LB is not available; therefore, we decided to use the starting date of the training dataset as 27 October 2010.
2. **During-COVID-19 pandemic period** is from 18 November 2019 to end of April 2021. For the beginning of the crisis, we follow the study of [Khanthavit \(2020\)](#). We perform this period with the aim of assessing comovement impact. Figure 2 shows that, as an example, one-month LB yields in all bond markets continual low yield pre-COVID-19 period, while Figure 3 shows that during-COVID-19 pandemic is comparative higher volatility than pre-COVID-19 pandemic in all bond markets. However, LB yields that have the higher tenor, the most likely less impact from the COVID-19 pandemic and, further, the yields almost recover to pre-COVID-19 period. Note that the last date of COVID-19 pandemic period is not the end of the pandemic. We cut off the dataset at the date of our writing.

Note also that bond yields are the daily change of the bond yield in basis point,  $r_t = (yield_t - yield_{t-1}) * 100$ . The abbreviations of basis point are normally expressed as "bps" or "bips".

Once all datasets were collected they were cleaned and split into pre-COVID-19 period (2411 daily observations) and during-COVID-19 period (348 daily observation) with the aim of data descriptive statistics analysis, see the descriptive statistics in Table 3 for pre-COVID-19 period and Table 4 for during-COVID-19 period.

The average range of the benchmark government bond yields are [-22,15] for Thailand, [-23,20] for the US, [-24,20] for the UK and [-31,28] for Japan. Interestingly, during the COVID-19 period, the only tenor that is less than 10 years, LB average yields have a negative value. otherwise, it seems to have no impact from the COVID-19 pandemic. This may imply that COVID-19 pandemic only impacts Thai bond market in short-term bond. However, we have to investigate further and can see in Section 7.

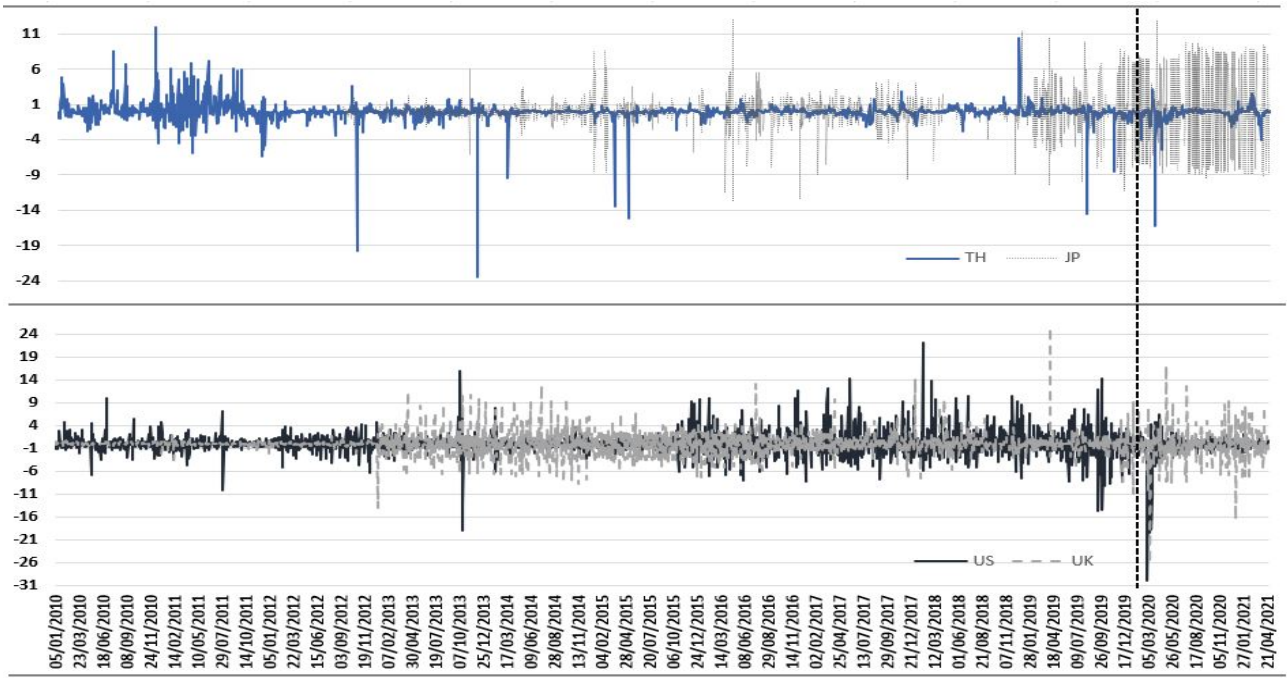
Figure 2: One-month government bond yields (%)



It is clear that, during the COVID-19 pandemic, funds flowed into the money market as low-risk securities, i.e., benchmark LB bonds in all bond markets. This is also confirmed by the negatively skewed distribution in all markets except Japan (positively skewed distribution). However, the COVID-19 crisis seems to affect short-term LB yields rather than long-term LB yields (LB that has the tenor greater or equal to 10 years). All LB bond markets during the COVID-19 pandemic, tend to have a lower yield, especially the lower tenor. Also, there are higher market fluctuations in all bond markets, again, except Japan. For kurtosis analysis, all bond markets have a leptokurtic distribution. This implied that all bond markets have heavy tails, especially the Thai bond market. Finally, we performed a JB test on both periods. In all bond market, JB test rejected the null hypothesis. Therefore, this implied that all benchmark LB yields are not normally distributed at the 99% confidence interval. Therefore, this justified the use of our proposed models in all bond markets and we will investigate them on bivariate



Figure 3: Example of one-month government bond yields (bps)



comovement analysis section.

Table 3: Descriptive statistics of pre-COVID-19 period dataset of benchmark government bond

	Government Bond (tenor)							
	Month			Year				
	1	3	6	1	5	10	20	30
<b>Pre-COVID-19 period dataset: 01/01/2010-17/11/2019</b>								
<b>Thailand</b>								
Min.	-23.49	-24.82	-25.96	-22.84	-19.76	-22.49	-15.08	-21.96
Max.	12.09	14.27	9.46	12.63	21.52	23.26	19.87	15.96
Mean	0.01	0.01	0.00	-0.01	-0.09	-0.11	-0.12	-0.08
Std.	1.32	1.35	1.35	1.35	2.75	3.21	2.36	2.01
Skewness	-4.50	-4.83	-6.22	-4.66	0.31	0.29	0.33	-1.18
Kurtosis	93.09	110.64	114.64	84.23	13.50	11.99	13.20	26.42
JB Test	823570***	1173279***	1267695***	671584***	11107***	8159***	10490***	51104***
Obs.	2411	2411	2411	2411	2411	2411	2411	2214
<b>United States of America</b>								
Min.	-19.00	-31.50	-8.80	-12.00	-21.60	-24.70	NA	-24.80
Max.	22.20	31.50	8.50	12.40	19.33	23.80	NA	26.20
Mean	0.06	0.06	0.06	0.05	-0.04	-0.08	NA	-0.08
Std.	2.32	1.81	1.37	1.66	4.72	5.08	NA	4.92
Skewness	0.76	0.13	-0.35	0.09	0.01	0.12	NA	0.17
Kurtosis	15.57	80.77	9.70	13.67	4.55	4.64	NA	5.40
JB Test	16109***	607530***	4553***	11438***	241***	275***	NA	542***
Obs.	2411	2411	2411	2411	2411	2411	NA	2214
<b>Unite Kingdom</b>								
Min.	-14.10	-17.80	-11.10	-26.00	-32.30	-28.80	-26.20	-24.40
Max.	25.40	21.00	8.70	28.90	34.20	21.20	15.80	15.80
Mean	0.01	0.01	0.01	0.00	-0.09	-0.13	-0.14	-0.13
Std.	2.03	1.36	1.22	3.64	4.45	4.91	4.28	4.12
Skewness	1.33	1.19	-0.37	-0.09	0.23	-0.01	-0.13	-0.10
Kurtosis	20.84	57.59	18.78	11.33	6.98	4.75	4.59	4.40
JB Test	32676***	299929***	25073***	6969***	1609***	306***	261***	185***
Obs.	2411	2411	2411	2411	2406	2411	2411	2214
<b>Japan</b>								
Min.	-12.80	-39.80	-35.50	-7.80	-19.60	-70.10	-16.50	-30.50
Max.	13.10	30.50	35.00	7.20	19.70	66.90	16.50	21.50
Mean	-0.01	-0.01	-0.01	-0.01	-0.03	-0.06	-0.07	-0.07
Std.	1.73	2.44	2.73	0.68	1.75	5.10	2.09	2.41
Skewness	-0.50	-3.10	0.04	0.49	0.32	-0.09	0.19	-0.71
Kurtosis	18.15	82.49	65.98	27.10	52.29	115.92	11.36	22.47
JB Test	16927***	545905***	398505***	58382***	243905***	1279982***	7034***	35127***
Obs.	1763	2062	2411	2214	2214	2214	2214	2214

*Note:* The minimum, maximum, mean and Std (standard deviation) are in bps unit. JB Test is the test statistic from Jarque-Bera's normality test. \*\*\* indicate the statistical significance at 1%. Obs. stands for number of observations. NA stands for no data available.

Table 4: Descriptive statistics of during-COVID-19 period dataset of benchmark government bond

	Government Bond (tenor)							
	Month			Year				
	1	3	6	1	5	10	20	30
<b>during-COVID-19 period dataset: 18/11/2019-30/04/2021</b>								
<b>Thailand</b>								
Min.	-16.23	-15.43	-15.11	-14.74	-18.35	-20.00	-12.06	-14.42
Max.	3.27	6.64	5.44	5.33	20.23	26.48	25.83	27.21
Mean	-0.28	-0.28	-0.26	-0.25	-0.11	0.04	0.16	0.24
Std.	1.20	1.28	1.24	1.22	3.31	4.21	3.84	2.90
Skewness	-7.20	-4.77	-5.05	-4.81	1.06	1.22	2.19	3.26
Kurtosis	92.46	61.66	64.28	63.27	13.60	12.80	15.79	33.52
JB Test	119063***	51213***	55922***	54019***	1696***	1479***	2650***	14125***
Obs.	348	348	348	348	348	348	348	348
<b>United States of America</b>								
Min.	-30.00	-24.70	-18.90	-18.90	-22.89	-27.30	-13.55	-31.00
Max.	6.40	7.90	6.10	11.00	23.10	32.90	15.50	39.10
Mean	-0.46	-0.44	-0.45	-0.43	-0.22	-0.06	0.47	0.00
Std.	3.01	2.90	2.57	2.44	4.48	5.55	4.40	6.21
Skewness	-4.91	-4.78	-4.41	-3.24	-0.23	0.04	0.10	-0.16
Kurtosis	38.84	33.88	28.85	23.76	10.91	10.23	4.13	11.74
JB Test	20025***	15153***	10822***	6860***	911***	757***	12***	1109***
Obs.	348	348	348	348	348	348	222	348
<b>Unite Kingdom</b>								
Min.	-26.10	-19.90	-21.90	-21.10	-14.20	-16.00	-26.80	-33.20
Max.	17.20	19.90	11.40	9.40	14.80	23.50	28.70	36.20
Mean	-0.19	-0.19	-0.20	-0.18	-0.05	0.01	0.03	0.01
Std.	3.65	3.54	3.36	2.94	3.29	4.03	4.90	5.25
Skewness	-0.87	-0.20	-1.30	-0.74	-0.03	0.63	0.08	0.16
Kurtosis	12.99	11.08	11.69	10.63	6.71	7.10	9.45	14.23
JB Test	1490***	949***	1194***	876***	199***	266***	603***	1829***
Obs.	348	348	348	348	348	348	348	348
<b>Japan</b>								
Min.	-11.20	-14.00	-16.40	-3.60	-5.00	-4.80	-5.70	-6.00
Max.	13.00	13.50	13.70	5.20	10.40	10.90	7.80	5.80
Mean	-0.02	0.06	0.02	0.02	0.02	0.04	0.04	0.05
Std.	5.47	3.21	2.83	0.84	1.31	1.36	1.49	1.63
Skewness	0.01	0.32	-0.43	0.64	1.48	1.45	0.12	-0.23
Kurtosis	2.32	9.26	9.36	10.78	16.03	15.61	5.93	4.52
JB Test	6***	573***	597***	901***	2591***	2428***	125***	36***
Obs.	348	348	348	348	348	348	348	348

*Note:* The minimum, maximum, mean and Std (standard deviation) are in bps unit. JB Test is the test statistic from Jarque-Bera's normality test. \*\*\* indicate the statistical significance at 1%. Obs. stands for number of observations.

## 6 Simulation result

This section shows the results of **(a)** the model parameter estimation of our proposed model such as in equations 4, 5 and 6 using the (Blocked-)QMLE estimation method. We developed the coding in MATLAB<sup>®</sup>. We then performed an example of parameter estimation of the bivariate dependence model using the copula functions from Table 1 and Table 2. The experiments were performed on a desktop computer with an Intel Core i7-9700 CPU, 3.00 GHz, and 32 GB RAM. The (blocked-)QMLE estimation method was performed by maximising the log-likelihood function and this optimisation method can be computed using *fmincon* function in MATLAB<sup>®</sup>.

### 6.1 Step 1: Univariate (Asymmetric-)GARCH model

We calculated MAD to assess the model performance. 100 simulations were generated with 1000 observations. The EGARCH(1,1,1)-Mixture model and LogGARCH(1,1)-Mixture model used the one-step-QMLE estimation method while GARCH(1,1)-Mixture model used the blocked-QMLE estimation method. We performed two-blocking for the GARCH(1,1)-Mixture model such that for the first blocking,  $\{\xi^L, \xi^U\}$  were estimated and for the second blocking the rest of parameters,  $\{\omega, \alpha, \nu\}$ , were estimated. Note that the simulation results in Table 5 are an average of 100 simulations. Overall, the means are close to the true parameters. The standard deviations (Std) are acceptable. The MADs are significant low. This implies that the variability of the QMLE estimation method is acceptable and it does not have a convergence issue of estimation. Unsurprisingly, the highest computing time is from the GARCH(1,1)-Mixture model because of the blocked-QMLE method. However, the computing time is low at approximately 2.98 seconds. Note that the standard deviation of the GARCH model is noticeably high and it should be taken into account when the empirical experiment is performed.

### 6.2 Step 2: Copula-based dependence measure

After the previous step, we then simply performed data standardisation,  $z_t = y_t/\sqrt{h_t}$  and estimated the copula parameter(s) of all copula candidates in Equation 7 and in Table 1. Finally, we selected the best fitting model using the model comparison as per the discussion in section 4 and calculated the copula-based dependence value as per the discussion in subsection 3.3.3. Examples of copula parameters and copula-based dependence values are the Gaussian copula using MATLAB<sup>®</sup> function and the BB4 copula which was developed by the researcher in Table 6.

Again, simulation results in Table 6 are from an average of 100 data simulations. All means of copula parameter(s) and copula-based dependence measures were closed to the true value. The standard deviations and MADs were both low and acceptable.

Table 5: Estimation and model comparison results from simulation experiment. Note that GARCH(1,1)-Mixture model use Blocked-QMLE method otherwise it is QMLE method.

Parameter	True Value	(Blocked-)QMLE		
		Mean	Std	MAD
<b>GARCH(1,1)-Mixture</b>				
$\xi^L$	0.0654	0.2427	0.4907	0.1773
$\xi^U$	0.3141	0.3818	0.2282	0.0677
$\omega$	0.0100	0.0681	94.8590	0.0581
$\alpha$	0.0180	0.0120	20.1381	0.0060
$\nu$	0.9700	0.9198	105.0157	0.0502
Computing time (seconds)			2.98	
<b>EGARCH(1,1,1)-Mixture</b>				
$\xi^L$	0.1500	0.1163	1.0534	0.0337
$\xi^U$	0.3500	0.3346	1.6846	0.0154
$\omega$	-0.1000	-0.0962	0.4147	0.0038
$\gamma$	-0.1200	-0.1220	5.9237	0.0020
$\delta$	0.1300	0.1251	1.7435	0.0049
$\nu$	0.9800	0.9776	0.5419	0.0024
Computing time (seconds)			2.22	
<b>LogGARCH(1,1)-Mixture</b>				
$\xi^L$	0.1500	0.1302	2.6361	0.0198
$\xi^U$	0.2800	0.2575	4.4875	0.0225
$\omega$	0.0320	0.0297	0.4340	0.0023
$\alpha^+$	0.0030	0.0033	0.1266	0.0003
$\alpha^-$	0.0530	0.0525	0.5661	0.0005
$\nu$	0.9600	0.9574	0.4878	0.0026
Computing time (seconds)			0.50	

Table 6: Example of QMLE estimation method of copula parameter and copula-based dependence measure,  $\tau$  and  $\rho_s$

Copula	Parameter	True Value	QMLE Method		
			Mean	Std	MAD
Gaussian*	$\rho$	0.24	0.238	0.031	0.002
Copula-based Dependence Measure	$\tau$	0.15	0.155	0.019	0.005
	$\rho_s$	0.23	0.230	0.028	0.000
Computing time (seconds)			0.022		
BB4**	$\theta$	0.10	0.097	0.373	0.003
	$\delta$	0.44	0.431	1.079	0.009
Copula-based Dependence Measure	$\tau$	0.18	0.184	0.016	0.004
	$\rho_s$	0.27	0.271	0.023	0.001
Computing time (seconds)			0.161		

*Note:* \* indicates calculation is based on MATLAB<sup>®</sup> function. \*\* indicates calculation is based on the researcher's calculation using MATLAB implementation.

## 7 Bivariate nonlinear comovement analysis on benchmark Thai government bond and developed bond market

This section presents the analysis of Thai bond market nonlinear comovement on benchmark LBs (1 month, 3 months, 6 months, 1 year, 5 years, 10 years, 20 years, 30 years) and developed bond markets including the US, UK and Japan. Note that no data is available for 20 years US government bond. The nonlinear comovement analysis, via a proposed Bivariate-Copula-EGARCH-Mixture model and the QMLE estimation method, consists of two periods, namely the pre-COVID-19 pandemic period, between January 2010 and 17 November 2019, and the period during the COVID-19 pandemic, between 18 November 2019 and April 2021 (referred to hereafter as the 'during-COVID-19 pandemic period'). Note that we follow the study of [Khanthavit \(2020\)](#) for the beginning of the COVID-19 pandemic. The aim of splitting the data is to compare nonlinear comovement before and during the pandemic. The results of the nonlinear copula-based comovement measure include Spearman's  $\hat{\rho}_s$  and Kendall's  $\hat{\tau}$ . The IFM method is applied and the methodology has been explained in the earlier section, see Section 3.2. In the empirical experiment, there are two steps in the IFM method, the details being as follows.

- 1 **Data standardization using univariate marginal model:** In this part we propose two candidates for the marginal model, namely the univariate GARCH-Mixture model and the univariate EGARCH-Mixture model in a conditional heteroskedasticity model. Given the proposed models, the best-fitting model will be selected on the basis of statistical information. Given best-fitting marginal model, data standardization would be computed for the next step of the nonlinear copula-based comovement measure. It is worth mentioning that the LogGARCH process cannot be generated because many of the residuals are equal to zero.
- 2 **Nonlinear copula-based comovement measurement:** Here we use 16 candidates for the bivariate copula function as shown in Section 3.3. QMLE parameter estimators are estimated for all candidates. Then, we select the best-fitting copula candidate using the statistical evidence. Finally, given the individual best-fitting copula function, nonlinear comovement can be computed. Note that we use one-day lag daily data for the US bond market, two-day lag daily data for the UK bond market and zero-day lag daily data for the Japanese bond market in this analysis as it shows higher historical correlation than the other lags and makes more sense in practice.

To simplify the Thai bond market analysis, the findings are presented in the following three subsections: the first subsection is a discussion of pre-COVID-19 pandemic comovement; the

second subsection is a discussion of during-COVID-19 pandemic comovement; and the last subsection is a discussion of the COVID-19 impact on Thai bond market comovement.

### 7.1 Pre-COVID-19 pandemic nonlinear comovement analysis

This subsection presents the numerical results and analysis of Thai bond market comovement before the COVID-19 pandemic.

Table 7 shows model parameter estimators of the proposed marginal models from Section 3.2.

Overall, the univariate EGARCH-Mixture model is statistically preferable to traditional GARCH-Mixture model as indicated by the AIC/BIC values and the log-likelihood value. Further, the KS statistical test confirms that EGARCH-mixture model is the preferable model. It confirms that all bonds are fat-tailed and non-normally distributed (as indicated by the  $\xi$  of the GPD distribution function). There are nine bonds that statistically fit the EGARCH-Mixture model: the 1Y, 5Y, 10Y, 20Y and 30Y UK bonds, the 5Y, 10Y and 30Y US bonds and the 5Y TH bond. The volatility persistence coefficient  $\nu$  could imply that the most stable bond market is Japan, followed in order of decreasing stability by Thailand, the UK and the US. In general, the majority of bonds have very high volatility persistence in both marginal models (coefficient is greater than 0.7), except for the 3M and 6M TH bonds, the 6M and 1Y US bonds, the 6M UK bond and the 10Y and 20Y JP bonds. However, the EGARCH-Mixture model has comparatively lower volatility persistence than the GARCH-Mixture model, except for the 1M, 6M and 1Y JP bonds, the 3M UK bond and the 30Y US bond. Fifteen bonds have negative shock asymmetry and seventeen bonds have positive shock asymmetry. The shock size  $\delta$  persistence is low (the average coefficient is 0.16) except for the 6M and 1Y UK bonds, the 1Y US bond, the 5Y, 10Y and 20Y TH bonds and the 10Y and 20Y JP bonds (where the shock size coefficient is greater than 0.4). For further numerical results, see Table 7.

Following step one of the IFM, we select the best marginal model fitting which is the EGARCH-Mixture process. Hence, we transform the yields into uniform distributions. Figure 4 and Figure 5 depict pairwise historical correlation yields and transformed yields via the EGARCH-Mixture model, respectively. Note that we test the transformed residual autocorrelation using the Ljung-Box test and the results see Table 8.

Further, Figure 5 shows the results of nonlinear comovement measure including estimated Spearman's  $\hat{\rho}_s$  and estimated Kendall's  $\hat{\tau}$  in matrix representation given by best fitting of 16 bivariate copula functions. Note that the US, UK and JP bond's tenor in column of the matrix representation is the same bond tenor as the LBs' tenor. The best copula candidate seen in Table 8 is given by minimising AIC (Table 9) and BIC (Table 10).



Given the nonlinear comovement measure in Figure 5 and the best copula fitting function in Table 8 according to the AIC value and BIC value, the following conclusions can be drawn.

Given Table 8 for the sake of the LB comparison, the best fitting copula function is in the BB copula family (23 bonds pairwise), i.e, the BB10 and BB9 copula function. The second best fitting function is the Frank copula in which there are five bonds pairwise that are the best fit to the Frank copula. This BB copula family presents asymmetric and different upper and lower tail dependence while the Frank copula presents symmetric and tail independence. This implies that there is asymmetric information in the Thai bond market. For comovement between LBs and developed market bonds, the Elliptical copula family is the most common best fit to the bond pairwise data (8 bonds pairwise). The Gaussian copula presents symmetric and no tail dependence while the Student's t copula presents symmetric and upper and lower tail dependence. There are two bonds pairwise that are best fit to the Clayton copula, where the Clayton copula presents asymmetric but only lower tail dependence.

For the sake of the comparison of the LB comovement measure, there is positive nonlinear comovement in all LBs. In the column vector (the comovement between the bond and its lower tenor bond), it is clear that the closer the bond tenor, the higher the nonlinear comovement. This is the so-called spillover effect. For example, the Spearman's  $\hat{\rho}_s$  of LB5Y with {LB1Y, LB6M, LB3M, LB1M} is {0.5997, 0.4724, 0.4180, 0.2966}, respectively. In the row vector (the comovement between the bond and its higher tenor bond), interestingly, the spillover effect is not clear but it is clearer in the long-term bonds (10Y 20Y 30Y LB). Otherwise, it is not clear there is a spillover effect. More precisely, there are differences in the order. For example, for LB1M, the order from highest comovement to lowest is LB3M, LB1Y, LB6M, LB20Y, LB10Y, LB5Y and LB30Y. For LB3M, the order from highest comovement to lowest is LB6M, LB1M, LB1Y, LB30Y, LB20Y, LB5Y and LB10Y. However, it is more likely that the closer the tenor, the higher the nonlinear comovement. See all numerical comovements in the Figure 5.

Lastly, we compare the nonlinear comovement measure between the Thai bond market and the developed bond market. We find that, overall, there is positive nonlinear comovement except in the 1M, 3M and 6M JP bond tenors and the 1M UK bond tenor which is a negative comovement (19 out of 23 bonds pairwise). The Thai bond market tends to have the highest positive comovement with the UK bond market, especially the bond tenor that is five years or more (five out of eight bonds pairwise). For the bond tenor that is lower than five years, the LB1Y that has the highest positive comovement is in the US bond market ( $\hat{\rho}_s = 0.4539, \hat{\tau} = 0.3094$ ). The LB6M that has highest positive comovement is in the UK bond market ( $\hat{\rho}_s = 0.4472, \hat{\tau} = 0.3052$ ), while the LB1M ( $\hat{\rho}_s = -0.2321, \hat{\tau} = -0.1557$ ) and LB3M ( $\hat{\rho}_s = -0.1977, \hat{\tau} = -0.1324$ ) that have the highest comovements, though these are negative,



Figure 4: Pre-COVID-19 period: Pairwise correlation of historical yields. US, UK, JP in the row representations are the 1-month, 3-month, 6-month, 1-year, 5-years, 10-year, 20-year and 30-year bonds, respectively. *Note:* NA indicates no data available.

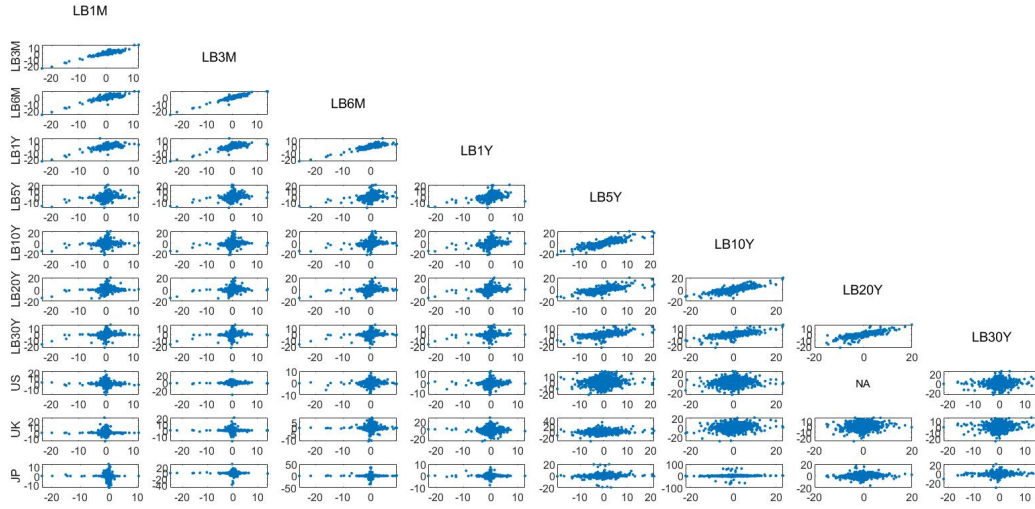
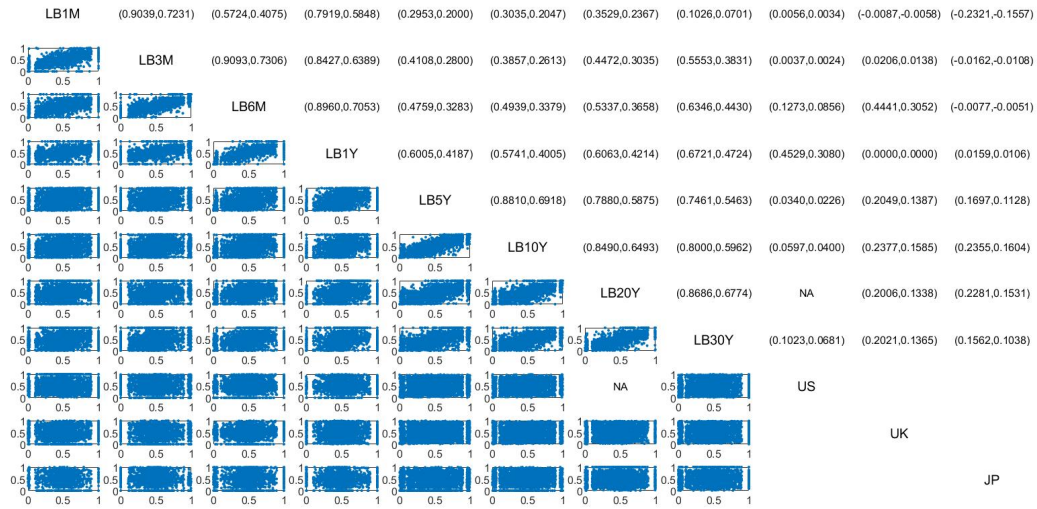


Figure 5: Pre-COVID-19 period: Transformed yields via EGARCH(1,1,1)-Mixture model prior to fitting a bivariate copula and its Spearman's  $\rho_s$  and Kendall's  $\hat{\tau}$ , respectively. US, UK, JP in the row representations are the 1-month, 3-month, 6-month, 1-year, 5-years, 10-year, 20-year and 30-year bonds, respectively. *Note:* NA indicates no data available.



## 7.2 During-COVID-19 pandemic nonlinear comovement analysis

This subsection presents the numerical results and analysis of the Thai bond market comovement during the COVID-19 pandemic.

Table 11 shows model parameter estimators of proposed marginal models from Section 3.2.

Overall, the univariate EGARCH-Mixture model is statistically preferable to the traditional

Table 8: Pre-COVID-19 period: Best bivariate copula candidate given by AIC/BIC values. *Note:* NA indicates no data available. \*\*\*, \*\*, \* indicate the statistical Ljung–Box test significance at 10%, 5%, 1% respectively. Ljung–Box test is statistical testing residual autocorrelation; Statistical significance of the Ljung–Box test showing in row representation of the US, UK and JP bond markets indicates that no autocorrelation. For example, 'Clayton\*' indicates the Ljung–Box test result with 1% significance level using the standard residual data of the 3M US bond.

	LB1M	LB3M	LB6M	LB1Y	LB5Y	LB10Y	LB20Y	LB30Y
LB3M	Frank							
LB6M	BB1	BB8						
LB1Y	BB10	BB10	BB10					
LB5Y	BB9	Frank	BB9	BB10				
LB10Y	Frank	BB10	BB10	BB10	Frank			
LB20Y	BB10	BB10	BB10	BB10	BB8	BB8		
LB30Y	BB1	BB10	BB10	BB10	Frank	BB8	BB8	
US	BB1	Clayton*	BB10	BB10	Clayton***	t**	NA	BB9*
UK	t	t	BB8	Gaussian	t***	BB9*	BB9	BB9
JP	Frank	Gaussian	Gaussian***	t	B5***	B5***	Frank**	BB1*

Table 9: Pre-COVID-19 period: AIC value of the best bivariate copula candidate. *Note:* NA indicates no data available.

	LB1M	LB3M	LB6M	LB1Y	LB5Y	LB10Y	LB20Y	LB30Y
LB3M	-3203.7							
LB6M	-2206.1	-3233.3						
LB1Y	-1389.9	-2105.8	-3422.8					
LB5Y	-130.5	-189.0	-312.7	-472.3				
LB10Y	-97.3	-133.0	-241.9	-379.9	-3096.7			
LB20Y	-96.6	-148.9	-244.7	-366.9	-1805.5	-2464.1		
LB30Y	-326.7	-244.7	-406.3	-468.8	-1290.3	-1675.0	-2463.7	
US	-263.7	0.2	-5.1	-34.2	0.2	-3.2	NA	-15.3
UK	-0.7	-44.2	-61.8	2.0	-80.4	-88.8	-62.8	-65.4
JP	-3.6	-0.3	1.4	-33.4	-49.2	-102.2	-66.1	-251.9

Table 10: Pre-COVID-19 period: BIC value of the best bivariate copula candidate. *Note:* NA indicates no data available.

	LB1M	LB3M	LB6M	LB1Y	LB5Y	LB10Y	LB20Y	LB30Y
LB3M	-3205.7							
LB6M	-2208.7	-3235.9						
LB1Y	-1392.5	-2108.5	-3425.4					
LB5Y	-133.1	-191.0	-315.3	-474.9				
LB10Y	-99.3	-135.6	-244.5	-382.5	-3098.7			
LB20Y	-99.2	-151.6	-247.3	-369.5	-1808.2	-2466.7		
LB30Y	-329.3	-247.2	-408.4	-471.6	-1292.3	-1677.6	-2466.4	
US	-266.4	-1.8	-7.7	-36.8	-1.8	-5.9	NA	-17.9
UK	-3.3	-46.8	-64.4	0.0	-83.0	-91.4	-65.4	-68.0
JP	-5.6	-2.3	-0.6	-36.0	-51.2	-104.2	-68.1	-254.5

GARCH-Mixture model as indicated by the AIC/BIC values and the log-likelihood value. Further, the KS statistical test confirms that the EGARCH-Mixture model is the preferable model. Again, it confirms that all bonds are fat-tailed and non-normally distributed. There are

24 bonds that statistically fit to the proposed marginal models; in the GARCH-Mixture model these are the 1M US bond, the 2M, 1Y, 5Y and 10Y JP bonds and the 30Y TH bond; and in the EGARCH-Mixture model the 1M, 5Y, 10Y, 20Y and 30Y US bonds, the 6M, 1Y, 5Y, 10Y and 20Y JP bonds, the 1Y, 5Y, 10Y, 20Y and 30Y UK bonds and the 5Y, 10Y and 20Y TH bonds. The volatility persistence coefficient  $\nu$  could imply that the most stable bond market is Japan, followed in order of decreasing stability by the US, the UK and Thailand. In general, all bonds have very high volatility persistence in both marginal models, except for the 1M, 6M and 1Y US bonds, the 1Y and 10Y JP bonds in the EGARCH-Mixture model. However, overall, the EGARCH-Mixture model has lower volatility persistence than the GARCH-Mixture model except in the Thai bond market. Eighteen bonds have negative shock asymmetry and 15 bonds have positive shock asymmetry. For further numerical results, see Table 11.

Given the nonlinear comovement measure in Figure 7 and the best copula fitting function in Table 12 according to the lowest AIC value in Table 13 and the lowest BIC value in Table 14, the following conclusions can be drawn.

Given Table 12 for the sake of the LB comparison, the best fit for bond pairwise data is the Gumbel copula function (12 out of 28 bonds pairwise). The second best is the BB10 (seven bonds pairwise), followed by the BB9 (six bonds pairwise) and the BB3 (two bonds pairwise). Almost all the best copula fit to the bond pairwise data during the COVID-19 pandemic belong to asymmetric and upper and lower tail dependence (27 out of 28 bonds pairwise). There is only one symmetric and tail independence copula best fit to the bond pairwise data, which is the Gaussian copula. This implies that there is asymmetric information in Thai bond market during the COVID-19 pandemic. For comovement between LBs and developed market bonds, the Elliptical copula family is the most common best fit to the bond pairwise data (symmetric and no tail dependence for the Gaussian copula (six out of 24 bonds pairwise) and upper and lower tail dependence for the Student's t copula (six out of twenty-four bonds pairwise)). There are two bonds pairwise that are symmetric and tail independent property which, are in the Frank copula. The rest of the bonds pairwise best copula fits are to the Gumbel, BB9, BB10, BB1 and Galambos copulas which all show asymmetric and different two-tail dependence.

For the sake of the comparison of the LB bond comovement measure, all LB bonds pairwise belong to positive nonlinear comovement. In the row vector (the comovement between the bond and its higher tenor bond), LBs bond pairwise with the tenor that is 6 months or more have a clearer spillover effect: the closer the tenor bonds pairwise, the higher the nonlinear comovement. For example, the Spearman's  $\hat{\rho}_s$  of LB1Y with {LB5Y, LB10Y, LB20Y, LB30Y} is {0.5480, 0.4862, 0.4510, 0.4206}, respectively, while, the Spearman's  $\hat{\rho}_s$  of LB1M with {LB3M, LB6M, LB1Y, LB5Y, LB10Y, LB20Y, LB30Y} is {0.9254, 0.8846, 0.8025, 0.6449, 0.4507, 0.4414,







Table 12: During-COVID-19 period: Best bivariate copula candidate given by AIC/BIC values. \*\*\*, \*\*, \* indicate the statistical Ljung–Box test significance at 10%, 5%, 1% respectively. Ljung–Box test is statistical testing residual autocorrelation; Statistical significance of the Ljung–Box test showing in row representation of the TH, US, UK and JP bond markets indicates that no autocorrelation. For example, 'BB9\*' indicates the Ljung–Box test result with 1% significance level using the standard residual data of the 10Y JP bond. 'LB5Y\*' indicates the Ljung–Box test result with 1% significance level using the standard residual data of the 5Y TH bond.

	LB1M	LB3M	LB6M	LB1Y	LB5Y*	LB10Y***	LB20Y	LB30Y
<b>LB3M</b>	Gumbel							
<b>LB6M</b>	BB10	BB10						
<b>LB1Y</b>	Gumbel	Gumbel	BB10					
<b>LB5Y</b>	BB10	BB3	Gaussian	BB3				
<b>LB10Y</b>	Gumbel	BB10	Gumbel	Gumbel	BB9			
<b>LB20Y</b>	Gumbel	BB10	Gumbel	Gumbel	BB10	BB9		
<b>LB30Y</b>	BB9	BB9	Gumbel	Gumbel	BB9	BB9	Gumbel	
<b>US</b>	Frank**	t	Frank	BB9	Gumbel***	Gumbel***	BB1	Galambos***
<b>UK</b>	Gaussian**	t**	Gaussian*	Gaussian***	t***	Gaussian***	t***	Gaussian***
<b>JP</b>	t	BB9***	Gumbel	t	BB1*	BB9*	BB10***	Gumbel***

Table 13: During-COVID-19 period: AIC value of best bivariate copula candidate.

	LB1M	LB3M	LB6M	LB1Y	LB5Y	LB10Y	LB20Y	LB30Y
<b>LB3M</b>	-614.3							
<b>LB6M</b>	-489.2	-569.8						
<b>LB1Y</b>	-317.2	-366.9	-613.1					
<b>LB5Y</b>	-132.0	-119.5	-106.6	-144.7				
<b>LB10Y</b>	-79.7	-84.2	-58.4	-86.2	-527.6			
<b>LB20Y</b>	-75.0	-78.1	-57.1	-73.4	-324.3	-444.5		
<b>LB30Y</b>	-88.5	-80.2	-49.4	-66.8	-199.5	-225.8	-254.5	
<b>US</b>	1.2	-0.1	-0.7	3.4	2.0	2.0	2.2	0.2
<b>UK</b>	0.2	7.0	0.5	-2.9	-17.3	-6.7	-23.9	-15.7
<b>JP</b>	16.4	2.5	2.0	5.1	-28.3	-50.7	-39.0	-4.2

Table 14: During-COVID-19 period: BIC value of best bivariate copula candidate.

	LB1M	LB3M	LB6M	LB1Y	LB5Y	LB10Y	LB20Y	LB30Y
<b>LB3M</b>	-616.3							
<b>LB6M</b>	-491.8	-572.4						
<b>LB1Y</b>	-319.2	-368.9	-615.7					
<b>LB5Y</b>	-134.6	-122.1	-108.6	-147.3				
<b>LB10Y</b>	-81.7	-86.8	-60.4	-88.2	-530.3			
<b>LB20Y</b>	-77.0	-80.7	-59.1	-75.4	-326.9	-447.1		
<b>LB30Y</b>	-91.1	-82.8	-51.4	-68.8	-202.1	-228.4	-256.5	
<b>US</b>	-0.8	-2.7	-2.7	0.8	0.0	0.0	-0.4	-1.8
<b>UK</b>	-1.8	4.4	-1.5	-4.9	-19.9	-8.7	-26.5	-17.7
<b>JP</b>	13.7	-0.1	0.0	2.5	-30.9	-53.3	-41.6	-6.2

### 7.3 COVID-19 impact on nonlinear comovement in Thai bond market

This subsection presents the analysis of the nonlinear comovement due to the impact of the COVID-19 pandemic in the Thai bond market.



Table 15 shows that Thai bond market characteristics have been changed in showing more extreme asymmetric and tail dependence during the COVID-19 pandemic. In the pre-COVID-19 pandemic analysis, BB10 is the majority copula best fit to the Thai bond pairwise data, while during the pandemic, the majority copula best fit changed to the Gumbel, which is in an extreme value copula family. Furthermore, number of bonds pairwise showing a best fit to Frank and Gaussian copula for the Thai bond market decreased from eleven to eight bonds pairwise (no tail dependence).

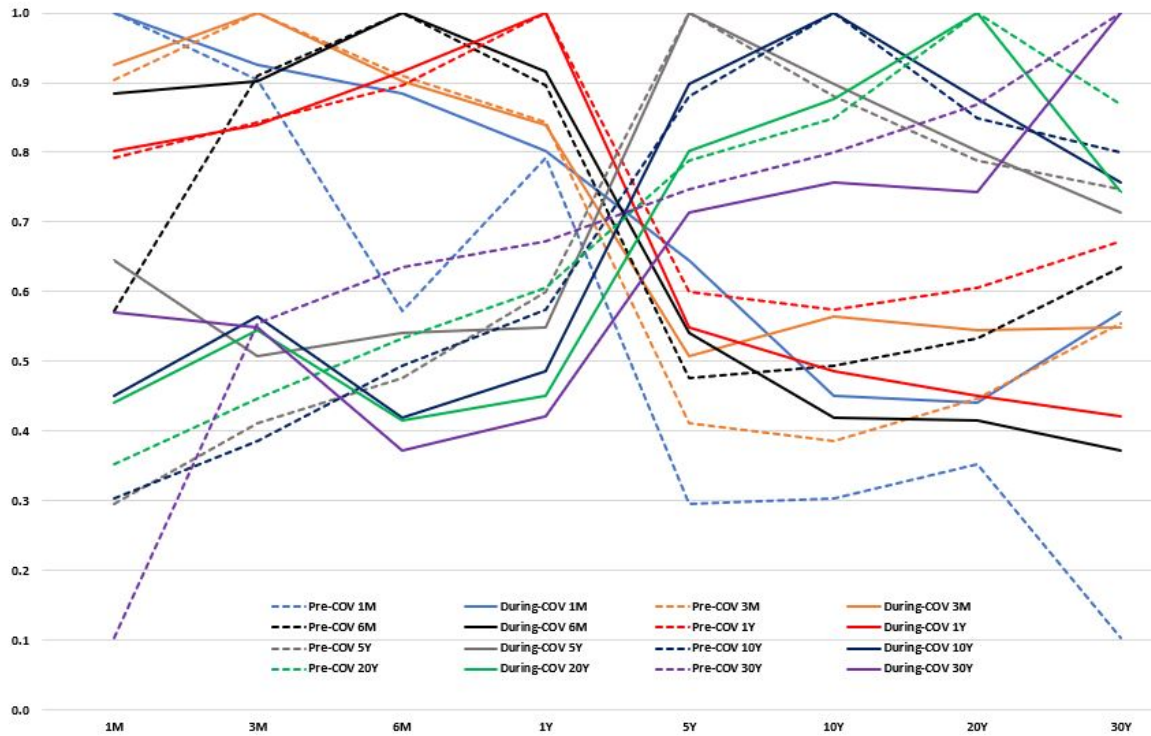
Given by Table 8 (pre-COVID-19 pandemic) and Table 12 (during-COVID-19 pandemic) and for the sake of the COVID-19 impact in nonlinear comovement in Thai market bonds, nine bonds pairwise have changed their best copula fit from BB10 to Gumbel. Three bonds pairwise have not changed their best copula fit and remain with BB10. Two bonds pairwise have changed their best copula fit from Frank to Gumbel. Two bonds pairwise have changed their best copula fit from BB8 to BB10. Two bonds pairwise have changed their best copula fit from BB8 to BB9. For the sake of the comparison of the LBs and developed market bonds in terms of the changing copula family point of view, the comovement between Thai bond market and the UK bond market is more likely to be symmetric and tail independent because of number of Gaussian copula best fits increased due to the pandemic. For the Thai bond market and the US bond market, short-term bond tends to have more symmetry and independence than long-term bonds, while comovement with the Japanese bond market has changed from no tail dependence to asymmetric and lower/upper tail dependence.

Table 15: Bivariate copula function best fitting to the Thai bond market. Note that the 20Y US Government bond data is not available for pre-COVID-19 pandemic period.

Bivariate Copula Function	Gaussian	Student's t	Frank	Clayton	Galambos	Gumbel	B5	BB1	BB3	BB8	BB9	BB10	Total
Pre-COVID-19	3	5	7	2	0	0	2	4	0	6	6	16	51
During-COVID-19	6	6	2	0	1	16	0	2	2	0	9	8	52

Figure 8 depicts Spearman's  $\hat{\rho}_s$  and Figure 9 depicts Kendall's  $\hat{\tau}$  in the Thai bond market (LBs only), both pre-COVID-19 pandemic and during-COVID-19 pandemic. Numerical nonlinear Spearman's  $\hat{\rho}_s$  and Kendall's  $\hat{\tau}$  comovement between LBs confirm that there is a spillover effect in both pre-COVID-19 pandemic and during-COVID-19 pandemic. More precisely, on the one hand, comovement between short-term bonds (1-month, 3-month, 6-month and 1-year LBs) are more likely to have high positive comovement rather than comovement between short-term and long-term bonds (5-, 10-, 20- and 30-year LBs). On the other hand, comovement between long-term bonds (5-, 10-, 20-, and 30-year LBs) are more likely to have high positive comovement. In general, Kendall's  $\hat{\tau}$  has a larger value than Spearman's  $\hat{\rho}_s$ . Besides, overall, both Spearman's  $\hat{\rho}_s$  and Kendall's  $\hat{\tau}$  for during-COVID-19 pandemic data seem to have higher values than for pre-COVID-19 pandemic data, especially in the short-term LBs. However,

Figure 8: Nonlinear Thai bond comovement: Comparison of Spearman's  $\hat{\rho}_s$  for the pre-COVID-19 period (dashed line) and during-COVID-19 period (solid line) in 1 month, 3 months, 6 months, 1 year, 5 years, 10 years, 20 years and 30 years LB tenors.



during the COVID-19 pandemic, comovement between long-term LBs and short-term LBs tends to be less than comovement in the pre-COVID-19 pandemic period.

Figure 10 depicts Spearman's  $\hat{\rho}_s$  between the Thai bond market and the developed bond markets, namely the US, UK and Japanese bond markets. Figure 11 depicts Kendall's  $\hat{\tau}$  between the Thai bond market and the developed bond markets, namely the US, UK and Japanese bond markets. Note that the 20-year US bond is not shown in either figure because no data is available. Figure 10 and Figure 11 show that, in general, nonlinear comovement during the COVID-19 pandemic decreases, especially for short-term bonds. For the pre-COVID-19 pandemic period, the Thai bond market seems to have more positive comovement with the UK bond market, especially for long-term bonds, while for short-term bonds, the Thai bond market has a high negative comovement with Japanese bond market. During the COVID-19 pandemic, comovement between the Thai bond market and the UK bond market tends to be reduced, while comovement with the Japanese bond market becomes positive but there is less comovement than in the pre-COVID-19 pandemic period. Further, comovement between the Thai bond market and all developed bond markets in the short-term is close to zeros, and this is also the case for the long-term US bond market.

Figure 9: Nonlinear Thai bond comovement: Comparison of Kendall's  $\hat{\tau}$  for the pre-COVID-19 period (dashed line) and during-COVID-19 period (solid line) in 1 month, 3 months, 6 months, 1 year, 5 years, 10 years, 20 years and 30 years LB tenors.

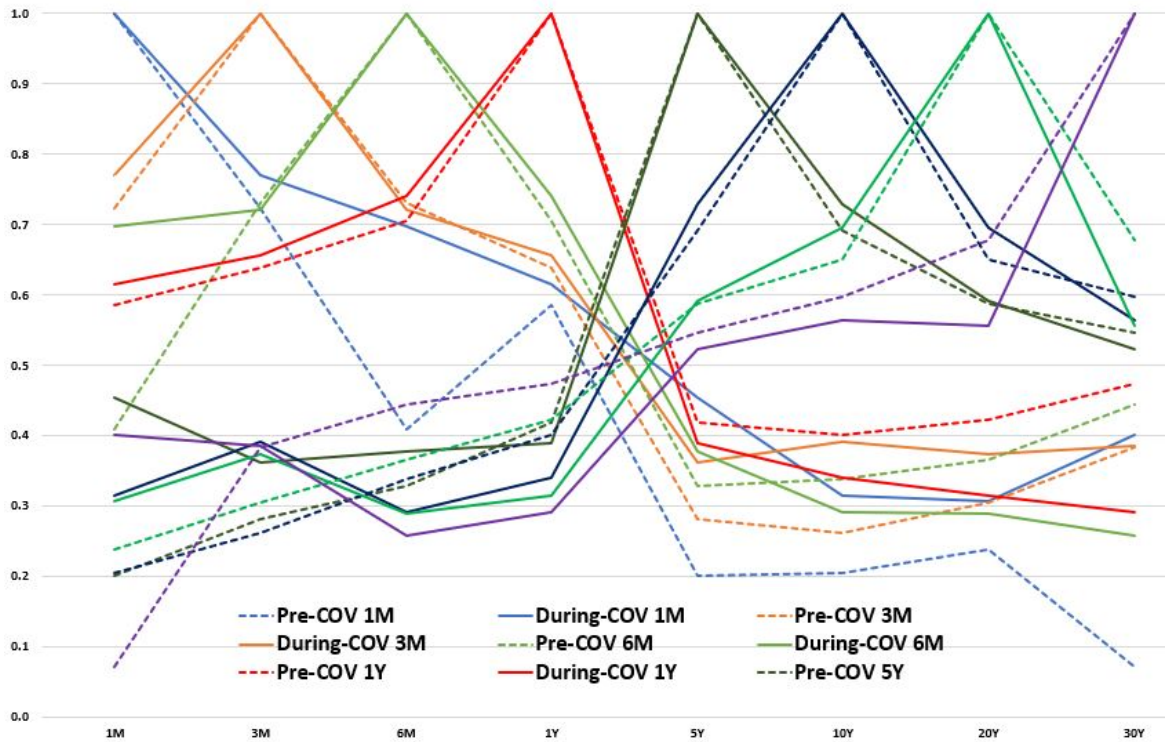


Figure 10: Nonlinear comovement between the Thai bond market and developed (US, UK Japanese) bond markets: Comparison of Spearman's  $\hat{\rho}_s$  for the pre-COVID-19 period (dashed line) and the during-COVID-19 period (solid line) in 1 month, 3 months, 6 months, 1 year, 5 years, 10 years, 20 years and 30 years bond tenors. Note that the bond tenor of all developed market bonds is equal to the LB's tenor.

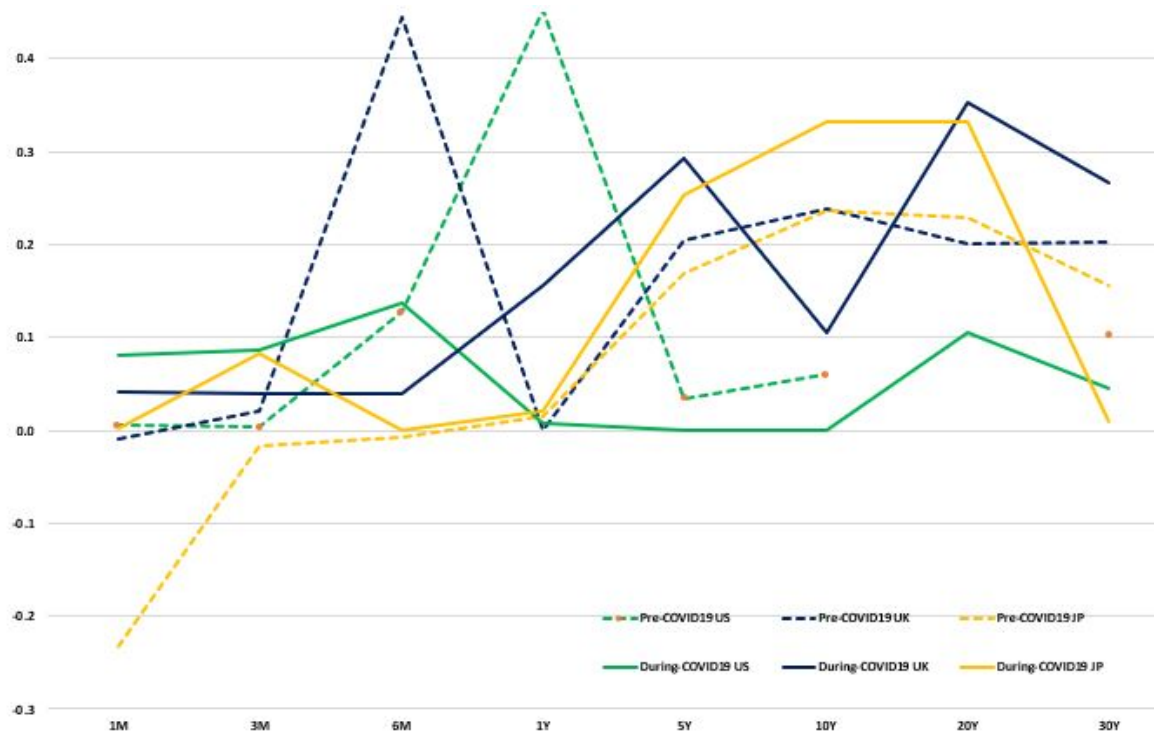
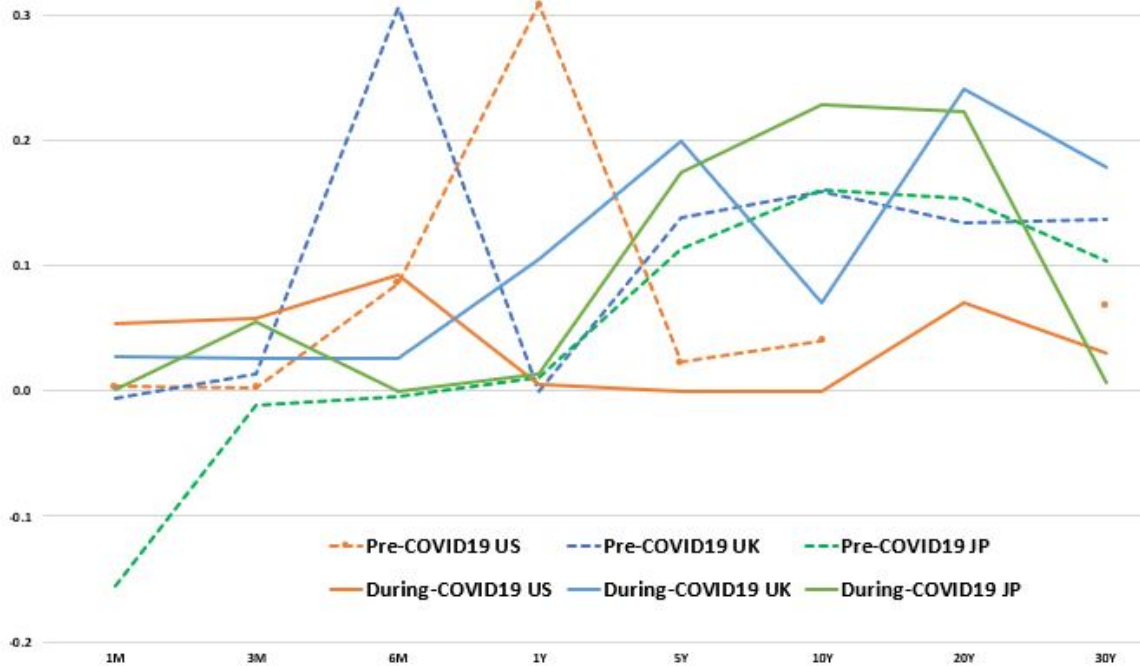


Figure 11: Nonlinear comovement between the Thai bond market and developed US UK Japanese bond market: Comparison of Kendall's  $\hat{\tau}$  for the pre-COVID-19 period (dashed line) and the during-COVID-19 period (solid line) in 1 month, 3 months, 6 months, 1 year, 5 years, 10 years, 20 years and 30 years bond tenors. Note that the bond tenor of all developed market bonds is equal to the LBs' tenor.



## 8 Policy implementation

Copula dependence function has been accepted widely in many areas, for instance, in insurance, civil engineer, medicine, climate and weather research and, especially, quantitative finance. In quantitative finance, copulas are mainly applied to quantitative risk management, portfolio allocation optimization and financial products pricing, in particular, derivatives pricing. Author will discuss two applications in policy implementation that related to role and responsibility of the bank of Thailand (BOT). Namely, it is financial risk measurement and Portfolio risk management.

**1 Risk measurement:** Typically, a measure of risk of financial products is an essential measure for both regulator and financial institute. Basically, the risk measure is Value-at-Risk (VaR) and Conditional-Value-at-Risk (CVaR). VaR estimates an amount of loss that investor might expect with a given probability. While CVaR is a risk measure that more conservative measure than VaR with a certain probability. Copula VaR and CVaR of bond can be easily measured by Monte Carlo simulation through, at a certain period of time of risk measure, the first step, expected bond yields can be generated by inverse cumulative distribution of proposed marginal model in Section 3.2 and Spearman's  $\hat{\rho}$  (or Kendall's  $\hat{\tau}$ ) in Figure 7 and, finally, bond VaR risk is a negative value of  $(1 - \alpha)$  percentile bond

yields, where  $\alpha$  is a confidence level, and bond CVaR risk is a negative value of an average of bond yields that below VaR at a certain confidence level.

**2 Portfolio risk optimization:** The measure of portfolio risk is also essential for both regulator and financial institute. This is still an active research area in modern finance, which also known as portfolio optimization problem. Variance-covariance ( $\Omega$ ) matrix is one of the most mechanism in portfolio theory. Basically,  $\Omega$  can be calculated by the traditional linear correlation in the Table ???. With this traditional correlation, it turns out standard and linear  $\Omega$ . Given copula bond yields generating by a Monte Carla simulation, copula  $\Omega$  can be easily calculated. It turns out a non-linear variance-covariance matrix. Indeed, it improves the measurement of portfolio risk in optimization problem. For further references see [Mathwork: Optimizing Market Risk using Copula Simulation](#) or Mathworks<sup>‡</sup>

Further, this study application is not limited to only the bond product. It could be applied to other financial products. Therefore, it can be contributed to the third roles and responsibilities of BOT, BOT's assets management. This study can, more or less, improve BOT's assets management for total portfolio return.

## 9 Conclusions and further research

This study reveals the impact of COVID-19 nonlinear comovement between the Thai bond market and the developed bond markets of the US, the UK and Japan using bivariate parametric copula. There are 16 candidates for bivariate parametric copula to fit these bond data and then measure nonlinear Spearman's  $\rho_s$  and Kendall's  $\tau$  comovement. The IFM method is adopted including data standardization using proposed EGARCH model with mixture innovation and then data fitting through bivariate parametric copula and, finally, nonlinear comovement measures.

It is clear that COVID-19 pandemic has impacted the comovement of Thai market bonds. The spillover effect of bond yield can be seen in the Thai bond market and it is clear in the short-term bond tenor. The comovement of LBs has changed to be more asymmetric and to show more extreme tail dependence. Moreover, comovement within the Thai bond market has tended to increase due to the impact of COVID-19, especially in the short-term LBs. Due to impact of COVID-19, Thai market bonds tend to independence, more symmetry and tail independence with developed market bonds. More precisely, short-term bond comovements have tended to decrease and are close to zero. However, long-term bond comovements tend to a small increase, especially in the Japanese bond market.

<sup>‡</sup>[https://www.mathworks.com/matlabcentral/mlc-downloads/downloads/submissions/42514/versions/4/previews/2\\_Analyze/html/copulaVaR.html](https://www.mathworks.com/matlabcentral/mlc-downloads/downloads/submissions/42514/versions/4/previews/2_Analyze/html/copulaVaR.html)

For further research, this study could be extended in many different directions, for example, by conducting a study using other estimation methods, such as the Bayesian Markov chain Monte Carlo (MCMC) method or the variational Bayesian method, in order to improve the parameter estimator. For the marginal model, conducting a study using other marginal models, for example, stochastic volatility model, may benefit data standardization. Using other complicated copula dependence models, a future study may use a multivariate copula model, for example, vine copula or factor copula. Finally, bond risk measures may use these copula models, for example var at risk or conditional value at risk.



## References

- Al Janabi, M. A. M., Arreola Hernandez, J., Berger, T., & Nguyen, D. K. (2017). Multivariate dependence and portfolio optimization algorithms under illiquid market scenarios. *European Journal of Operational Research*, *259*(3), 1121–1131.
- Ardia, D., Bluteau, K., Boudt, K., & Catania, L. (2018). Forecasting risk with markov-switching garch models: a large-scale performance study. *International Journal of Forecasting*, *34*(4), 733–747.
- Babaei, S., Sepehri, M. M., & Babaei, E. (2015). Multi-objective portfolio optimization considering the dependence structure of asset returns. *European Journal of Operational Research*, *244*(2), 525–539.
- Bauwens, L., Preminger, A., & Rombouts, J. V. K. (2010). Theory and inference for a markov switching garch model. *The Econometrics Journal*, *13*(2), 218–244.
- Berger, T. (2013). Forecasting value-at-risk using time varying copulas and evt return distributions. *International Economics*, *133*, 93–106.
- Bernardi, M., & Catania, L. (2018). Portfolio optimisation under flexible dynamic dependence modelling. *Journal of Empirical Finance*, *48*, 1–18.
- Bildirici, M., & Ersin, Ö. Ö. (2009). Improving forecasts of garch family models with the artificial neural networks: An application to the daily returns in istanbul stock exchange. *Expert Systems with Applications*, *36*(4), 7355–7362.
- Billio, M., Casarin, R., & Osuntuyi, A. (2016). Efficient gibbs sampling for markov switching garch models. *Computational Statistics and Data Analysis*, *100*, 37–57.
- Bollerslev, T. (1986). Generalized autoregressive conditional heteroskedasticity. *Journal of Econometrics*, *31*(3), 307–327.
- Breymann, W., Dias, A., & Embrechts, P. (2003). Dependence structures for multivariate high-frequency data in finance. *Quantitative Finance*, *3*(1), 1–14.
- Cai, J. (1994). A markov model of switching-regime arch. *Journal of Business and Economic Statistics*, *12*(3), 309–316.
- Chang, C., McAleer, M., & Wong, W. (2018). Big data, computational science, economics, finance, marketing, management, and psychology: Connections. *Journal of Risk and Financial Management*, *11*(1).
- Christiansen, C. (2007). Volatility-spillover effects in european bond markets. *European Financial Management*, *13*(5), 923–948.
- Creal, D. D., & Tsay, R. S. (2015). High dimensional dynamic stochastic copula models. *Journal of Econometrics*, *189*(2), 335–345.

- Czado, C. (2013). Vine copulas and their applications to financial data. *Actuarial and Financial Mathematics Conference*.
- De Lira Salvatierra, I., & Patton, A. J. (2015). Dynamic copula models and high frequency data. *Journal of Empirical Finance*, *30*, 120–135.
- Engle, R. (2004). Risk and volatility: Econometric models and financial practice. *The American Economic Review*, *94*(3), 405–420.
- Fan, Y., & Patton, A. J. (2014). Copulas in econometrics. *Annual Review of Economics*, *6*, 179–200.
- Fengler, M. R., & Okhrin, O. (2016). Managing risk with a realized copula parameter. *Computational Statistics and Data Analysis*, *100*, 131–152.
- Francq, C., Wintenberger, O., & Zakoïan, J. M. (2013). Garch models without positivity constraints: Exponential or log garch? *Journal of Econometrics*, *177*(1), 34–46.
- Francq, C., Wintenberger, O., & Zakoïan, J. M. (2018). Goodness-of-fit tests for log-garch and egarch models. *TEST*, *27*(1), 27–51.
- Glosten, L., Jagannathan, R., & Runkle, D. (1993). On the relation between the expected value and the volatility of the nominal excess return on stocks. *The journal of finance*, *48*(5), 1779–1801.
- Goel, A., Sharma, A., & Mehra, A. (2019). Robust optimization of mixed cvar starr ratio using copulas. *Journal of Computational and Applied Mathematics*, *347*, 62–83.
- Gray, S. F. (1996). Modeling the conditional distribution of interest rates as a regime-switching process. *Journal of Financial Economics*, *42*(1), 27–62.
- Hafner, C. M., & Kyriakopoulou, D. (2019). Exponential-type garch models with linear-invariance risk premium. *Journal of Business and Economic Statistics*, 1–15.
- Hamilton, J. D., & Susmel, R. (1994). Autoregressive conditional heteroskedasticity and changes in regime. *Journal of Econometrics*, *64*(1-2), 307–333.
- Hentschel, L. (1995). All in the family nesting symmetric and asymmetric garch models. *Journal of Financial Economics*, *39*(1), 71–104.
- Joe, H. (2015). “Dependence modelling with copulas”. CRC Press.
- Jose Rodriguez, M., & Ruiz, E. (2012). Revisiting several popular garch models with leverage effect: Differences and similarities. *10*, 637–668.
- Kakouris, I., & Rustem, B. (2014). Robust portfolio optimization with copulas. *European Journal of Operational Research*, *235*(1), 28–37.
- Karmakar, M., & Paul, S. (2018). Intraday portfolio risk management using var and cvar: A cgarch-evt-copula approach. *International Journal of Forecasting*.



- Khanthavit, A. (2020). “(covid-19)-induced flight to quality”. <https://doi.org/10.13140/RG.2.2.11384.88328>
- Li, F., & Kang, Y. (2018). Improving forecasting performance using covariate-dependent copula models. *International Journal of Forecasting*, *34*(3), 456–476.
- Massey, F. J. (1951). The kolmogorov-smirnov test for goodness of fit. *Journal of the American Statistical Association*, *46*(253), 68–78.
- McNeil, A. J., Frey, R., & Embrechts, P. (2015). “Quantitative risk management: Concepts, techniques and tools”. Princeton: Princeton University Press.
- Nelson, D. B. (1991). Conditional heteroskedasticity in asset returns: A new approach. *Econometrica*, *59*(2), 347–370.
- Neumeyer, N., Omelka, M., & Hudecová, Š. (2019). A copula approach for dependence modeling in multivariate nonparametric time series. *Journal of Multivariate Analysis*, *171*, 139–162.
- Oh, D. H., & Patton, A. J. (2016). High-dimensional copula-based distributions with mixed frequency data. *Journal of Econometrics*, *193*(2), 349–366.
- Patton, A. J. (2012). A review of copula models for economic time series. *Journal of Multivariate Analysis*, *110*, 4–18.
- Sahamkhadam, M., Stephan, A., & Östermark, R. (2018). Portfolio optimization based on garch-evt-copula forecasting models. *International Journal of Forecasting*, *34*(3), 497–506.
- Salman Khan, M., Khan, K., Mahmood, S., & Sheeraz, M. (2019). Symmetric and asymmetric volatility clustering via garch family models: An evidence from religion dominant countries.
- Segnon, M., & Trede, M. (2018). Forecasting market risk of portfolios: Copula-markov switching multifractal approach. *The European Journal of Finance*, *24*(14), 1123–1143.
- Sklar, M. (1959). Fonctions de repartition an dimensions et leurs marges. *Publ. inst. statist. univ. Paris*, *8*, 229–231.
- So, M. K. P., & Yeung, C. Y. T. (2014). Vine-copula garch model with dynamic conditional dependence. *Computational Statistics Data Analysis*, *76*, 655–671.
- Sucarrat, G., Gronneberg, S., & Escribano, A. (2016). Estimation and inference in univariate and multivariate log-garch-x models when the conditional density is unknown. *100*, 582–594.
- Weiβ, G. N. F., & Supper, H. (2013). Forecasting liquidity-adjusted intraday value-at-risk with vine copulas. *Journal of Banking and Finance*, *37*(9), 3334–3350.

World Bank. (2020). “The global economic outlook during the covid-19 pandemic: A changed world”.

Zakoian, J.-M. (1994). Threshold heteroskedastic models. *Journal of Economic Dynamics and Control*, 18(5), 931–955.